

NOTICE CONCERNING COPYRIGHT RESTRICTIONS

This document may contain copyrighted materials. These materials have been made available for use in research, teaching, and private study, but may not be used for any commercial purpose. Users may not otherwise copy, reproduce, retransmit, distribute, publish, commercially exploit or otherwise transfer any material.

The copyright law of the United States (Title 17, United States Code) governs the making of photocopies or other reproductions of copyrighted material.

Under certain conditions specified in the law, libraries and archives are authorized to furnish a photocopy or other reproduction. One of these specific conditions is that the photocopy or reproduction is not to be "used for any purpose other than private study, scholarship, or research." If a user makes a request for, or later uses, a photocopy or reproduction for purposes in excess of "fair use," that user may be liable for copyright infringement.

This institution reserves the right to refuse to accept a copying order if, in its judgment, fulfillment of the order would involve violation of copyright law.

GRAVITY MEASUREMENTS IN THE
AREA OF MOUNT HOOD, OREGON

By

RICHARD COUCH
MICHAEL GEMPERLE

Geophysics Group

School of Oceanography

Oregon State University

May 1979

Final report of work carried out under OSU Grant No. 30-262-9117 from the Oregon Department of Geology and Mineral Industries; July 1977 through March 1979.

GTR 790517

TABLE OF CONTENTS

	Page
ABSTRACT.....	142
GRAVITY ANOMALIES IN THE AREA OF MOUNT HOOD, OREGON.....	143
Gravity Measurements.....	143
Reduction of the Gravity Measurements.....	148
Free-Air Gravity Anomalies.....	150
Bouguer Gravity Anomalies.....	152
Regional Gravity Anomalies.....	161
MODELS OF MOUNT HOOD.....	169
ELEVATION OF THE COLUMBIA RIVER BASALT.....	176
POROSITY ESTIMATES.....	181
TRAVEL TIME RESIDUALS.....	185
ACKNOWLEDGEMENTS.....	187
REFERENCES.....	188
APPENDIX.....	189

LIST OF FIGURES

	Page
1 TOPOGRAPHIC MAP OF MOUNT HOOD.....	144
2 GRAVITY STATION LOCATION MAP.....	146
3 FREE-AIR GRAVITY ANOMALY MAP OF MOUNT HOOD.....	151
4 COMPLETE BOUGUER GRAVITY ANOMALY MAP OF MOUNT HOOD. REDUCTION DENSITY 2.67 gm/cm ³	153
5 GRAPH OF THE STANDARD DIVIATION OF THE COMPLETE BOUGUER ANOMALIES VERSUS THE COMPLETE BOUGUER REDUCTION DENSITY.....	155
6 COMPLETE BOUGUER GRAVITY ANOMALY MAP OF MOUNT HOOD. REDUCTION DENSITY 2.27 gm/cm ³	156
7a COMPLETE BOUGUER GRAVITY ANOMALY MAP: TIMBERLINE AREA. REDUCTION DENSITY 2.67 gm/cm ³	160
7b COMPLETE BOUGUER GRAVITY ANOMALY MAP: TIMBERLINE AREA. REDUCTION DENSITY 2.27 gm/cm ³	160
8 REGIONAL GRAVITY ANOMALY MAP OF THE MOUNT HOOD AREA: >13 km/cycle.....	163
9 RESIDUAL GRAVITY ANOMALY MAP OF THE MOUNT HOOD AREA: < 13 km/cycle.....	164
10 REGIONAL GRAVITY ANOMALY MAP OF THE MOUNT HOOD AREA: > 8.1 km/cycle.....	165
11 RESIDUAL GRAVITY ANOMALY MAP OF THE MOUNT HOOD AREA: < 8.1 km/cycle.....	167
12 SPHERE MODEL CONSISTENT WITH MOUNT HOOD GRAVITY ANOMALIES.....	170
13 CYLINDRICAL CORE MODEL OF MOUNT HOOD.....	171
14 CYLINDER AND CONE MODEL CONSISTENT WITH MOUNT HOOD GRAVITY ANOMALIES.....	173
15 DENSITY CONTRAST VERSUS RADIUS FOR CYLINDER AND CONE MODEL.....	174
16 ESTIMATED ELEVATION OF THE COLUMBIA RIVER BASALTS....	178
17 COMPARISON OF MAPPED AND COMPUTED PRE-PLIOCENE TOPOGRAPHIC SURFACE.....	180
18 ESTIMATED POROSITIES IN MOUNT HOOD AREA.....	183

LIST OF FIGURES (Con't.)

Page

19	ESTIMATED SEISMIC WAVE TRAVEL-TIME RESIDUALS IN MOUNT HOOD AREA.....	186
----	---	-----

LIST OF TABLES

	Page
1 APPENDIX.....	189
2 ANDESITE DENSITIES AND VELOCITIES.....	181

ABSTRACT

The analysis of gravity measurements at 337 stations on and about Mount Hood indicate lateral and vertical variations in the density of the flows and pyroclastics in and beneath Mount Hood. Complete Bouguer gravity anomalies indicate that the axis of Mount Hood is located on an elongate gravity high, oriented approximately N75E. Mount Hood is superimposed on a gravity low that extends from north of the mountain to the southern extent of the survey area. The gravity low suggests a north-south oriented graben-like structure. Prominent lineations in the gravity anomalies oriented approximately N23W occur both northwest and southwest of Mount Hood. A simple cone-on-a-cylinder model for the core of Mount Hood agrees with the gravity anomalies. Long wavelength anomalies suggest that undulations in the Columbia River Basalts beneath and about Mount Hood range from less than 500 m to over 1400 m above sea level. Porosities of the average rocks which comprise Mount Hood are estimated to be approximately 20 to 30 percent and the density is approximately 2.27 gm/cm^3 .

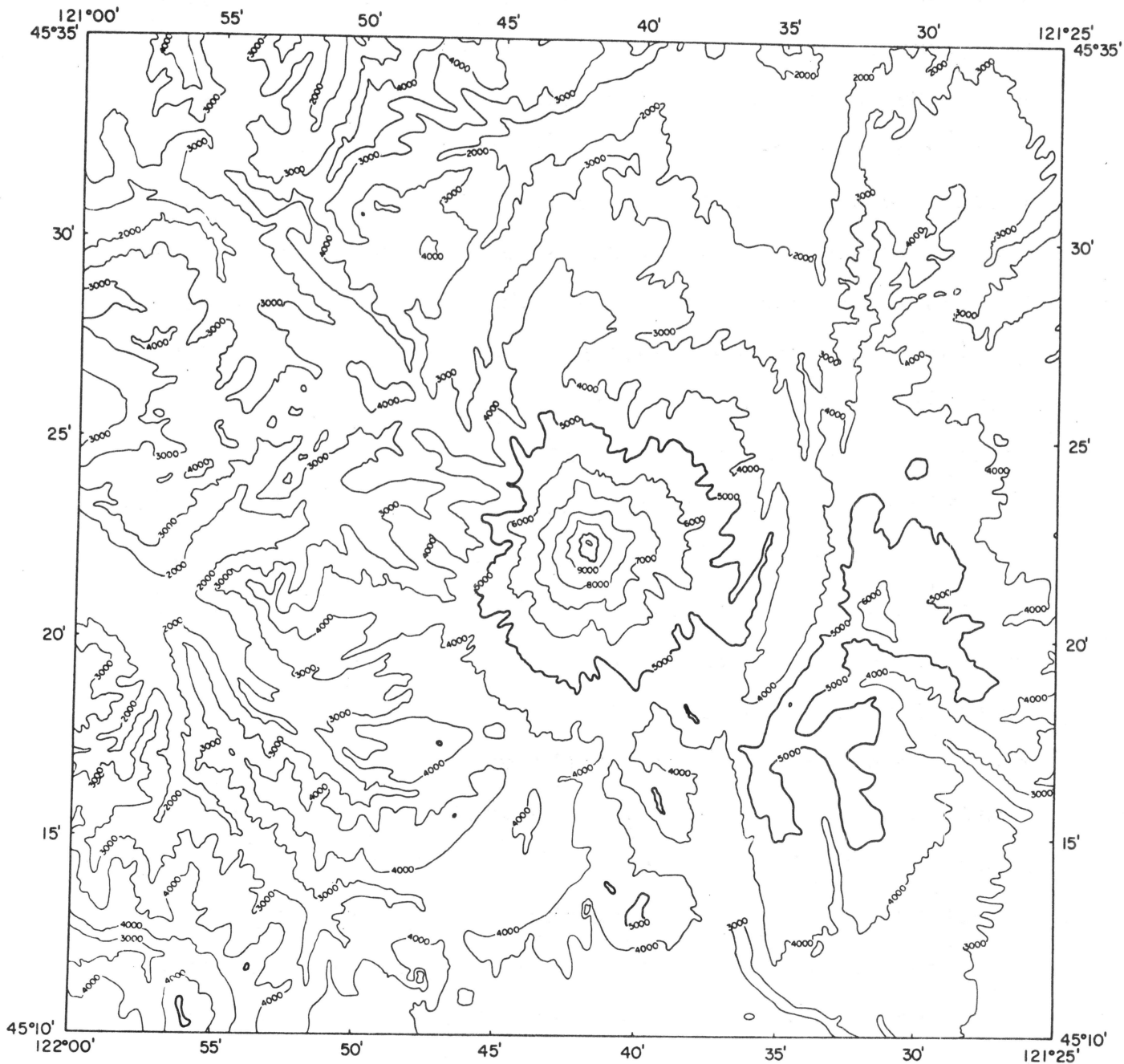
GRAVITY ANOMALIES IN THE AREA
OF MT. HOOD, OREGON

Gravity Measurements

Personnel of the Geophysics Group, Oregon State University (OSU) conducted a gravity survey in the High Cascade Mountains of northern Oregon during August and September, 1977 and August and September, 1978. The survey area which extends from $45^{\circ}10'$ to $45^{\circ}35'N$ lat. and from $121^{\circ}25'$ to $122^{\circ}00'W$ long. includes the picturesque 3424 m (11235 ft) high Mt. Hood strato-volcano and many surrounding foothills and mountains of the Cascade Range.

Figure 1 shows a topographic map of the area of and about Mt. Hood based on data contained on the U. S. Geological Survey (USGS) 1:250,000 quadrangle map, The Dalles NL 10-9. The map, contoured at an interval of 1000 ft (304.8 m), shows approximately 10,000 ft (3050 m) of topographic relief in the area of Mt. Hood. Mt. Hood, a relatively symmetric volcanic cone of Late Pleistocene to Holocene age, is surrounded by a north-south trending ridge over 6000 ft (1830 m) in elevation on the east and southeast side and isolated mountains and dissected ridges on the south, west, and northwest sides. Mt. Hood is composed almost entirely of pyroxene andesite and rises 8000 ft (2400 m) above a platform of Pliocene andesites and basalts (Wise, 1969). The high relief and few roads make access to the area difficult; consequently to achieve an approximately uniform grid of gravity stations most measurements were made by back-packing the meter to the station sites.

Mr. Kenneth Keeling, with the assistance of Messieurs.

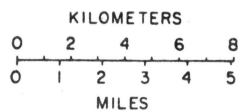


TOPOGRAPHIC MAP
MOUNT HOOD AREA, OREGON



AREA OF THIS MAP

DATA FROM USGS 1:250,000 QUADRANGLE MAP
THE DALLES NL 10-9



UNIVERSAL TRANSVERSE MERCATOR PROJECTION
CONTOUR INTERVAL 1000 FEET

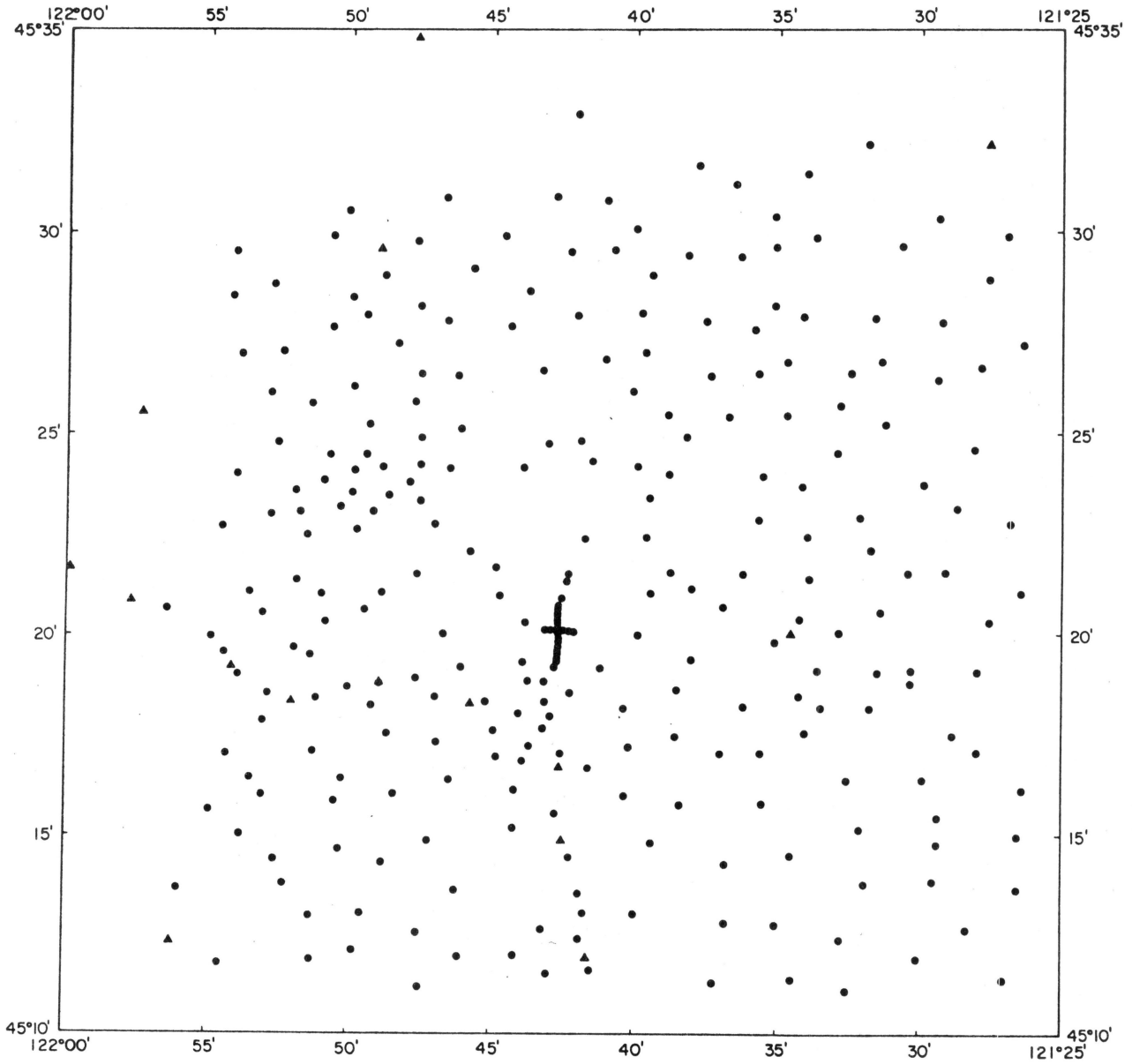
OREGON STATE UNIVERSITY
DECEMBER, 1977

Figure 1

Terry Jones, William Plank, and Mark Brown obtained gravity measurements at 239 stations in the approximately 2000 km² area. Messieurs. Gordon Ness and John Bowers established 51 closely spaced gravity stations in the vicinity of the geothermal test hole south southeast of Timberline Lodge (3S/9E-7ca) on the south slope of Mt. Hood and added an additional 33 stations to the area survey. These stations, combined with station data from the Oregon State University Library (Thiruvathukal, 1968), total 337 and yield an approximate spatial density of one station per 6 km².

Figure 2 shows the locations of the 337 gravity stations in the Mt. Hood survey area. In addition to the approximately uniform scatter of stations in the area, a high concentration of stations which form a plus sign near the middle of the map, occur along lines which extend north, south, east and west from a point near the site of the geothermal test hole. Gravity stations are concentrated also toward the south and west along Highway U. S. 26 on the south flank of Mt. Hood. A solitary gravity station is located on the summit of Mt. Hood.

Base stations for the measurements were established at Zigzag Ranger Station, Government Camp, White Bridge Park, Parkdale, and near Cooper Spur. The Zigzag Ranger Station gravity base station (980,489.14 mgl) was tied to the USAF gravity base station WA-142A (Woollard and Rose, 1963) located at Portland International Airport (980,648.3 mgl) by personnel of the USGS (personnel comm. D. G. Barnes, 1969) and by the personnel of the OSU Geophysics Group (unpublished data, OSU Gravity Library, 1975). The detailed survey near Timberline



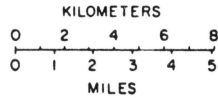
GRAVITY STATIONS
MOUNT HOOD AREA, OREGON



AREA OF 1:5 MAP

GRAVITY STATIONS

- ▲ J. THIRUVATHUKAL . 1969 OSU
- K. KEELING 1977 OSU
- G. NESS & J. BOWERS 1978 OSU



UNIVERSAL TRANSVERSE MERCATOR PROJECTION

OREGON STATE UNIVERSITY
DECEMBER, 1978

Figure 2

Lodge is referenced to the gravity base station at Zigzag Ranger Station. The measurements were made with a LaCoste and Romberg Model G Geodetic Gravity Meter #126.

USGS benchmarks, spot elevations on USGS 7.5 minute and 15 minute topographic maps and barometric altimetry provided vertical control for the gravity stations. The estimated uncertainties in the vertical control associated with these methods of elevation determination are ± 1 , ± 5 , and ± 10 feet respectively. A recording barometer base station, used to monitor barometric changes during the survey, provided data to ascertain the validity and accuracy of altitudes determined by barometric altimetry.

USGS 7.5 minute and 15 minute topographic maps were used to determine horizontal position. The estimated uncertainty in horizontal position is ± 0.02 minutes of latitude and longitude. MSS Inc., Corvallis, established reference points for the gravity stations near the geothermal drill site. The positions and elevations of the detailed gravity survey, determined by triangulation and leveling techniques, were established with reference to a USGS benchmark at Timberline Lodge. The estimated uncertainty is less than ± 0.3 meters in the horizontal position of each station and less than ± 0.3 meters in the vertical elevation of each station with respect to the USGS benchmark.

The observed gravity was corrected for earth tides using the formulation of Longman (1959) and for meter drift by linear interpolation between values observed at reoccupied base stations. The mean drift of the gravity meter observed during

reoccupation of base stations at the end of a gravity traverse or loop was ± 0.04 mgl and the standard deviation was 0.09 mgl. The maximum observed drift was 0.47 mgl. The uncertainties in the measurements caused by the drift of the meter is generally much less than caused by the uncertainties in the corresponding station elevations.

Reduction of the Gravity Measurements

The gravity measurements were reduced to free-air and complete Bouguer gravity anomalies with standard techniques. The following equation from Scheibie and Howard (1964) and Oliver (1973), used in this study, yields the free-air gravity anomaly:

$$\text{FAA} = \text{OG} - \text{THG} + (0.09411549 - 0.000137789 \sin^2 \theta)h - 0.67 \times 10^{-8} h^2$$

where,

FAA = Free-air anomaly in milligals

OG = Observed gravity in milligals

THG = Theoretical gravity in milligals

θ = Latitude

h = Elevation in feet

The International Gravity Formula (IGF), yields theoretical gravity (THG) values at designated latitudes. The IGF of 1930 (Swick, 1942), used in this study, is:

$$\text{THG} = 978049.0 (1 + .0052884 \sin^2 \phi - 0.0000059 \sin^2 2\phi)$$

The following equation yields the complete Bouguer gravity anomaly (CBA).

$$\text{CBA} = \text{FAA} - 2\pi G \rho h + \text{TCC} - \text{CC}$$

where,

CBA = Complete Bouguer gravity anomaly in milligals

FAA = Free-air gravity anomaly in milligals

and $G =$ Universal gravitational constant
(6.67×10^{-8} cgs)

$p =$ Reduction density in gm/cm^3

$h =$ Elevation in feet

TTC = Total terrain correction in milligals

CC = Curvature correction = $hp (1.671 \times 10^{-8} +$
 $h[-1.229 \times 10^{-8} + h(4.76 \times 10^{-16})]$ milligals
(Oliver, 1973)

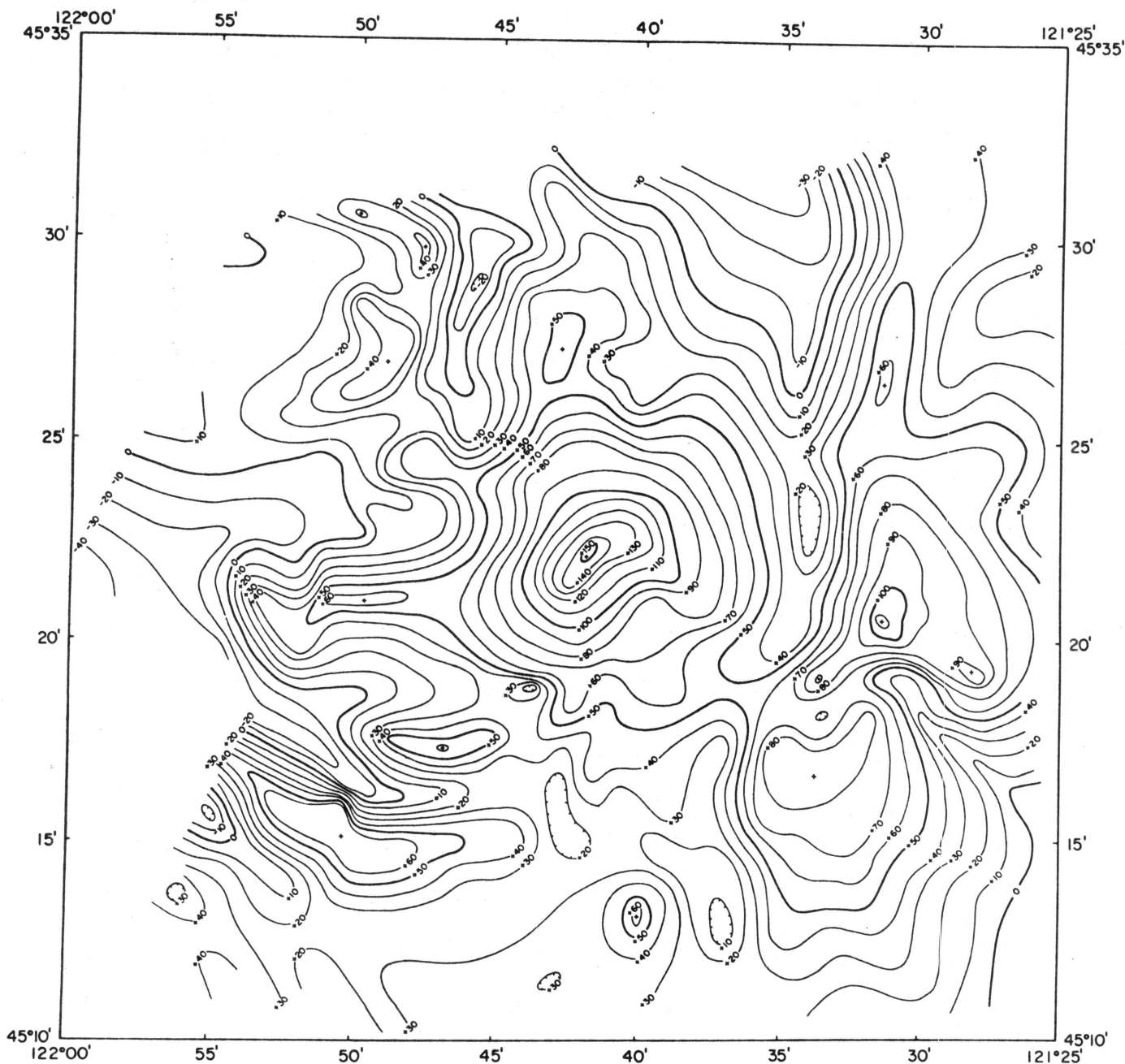
Terrain corrections for each station account for the change in gravity caused by topography about the station. Total terrain corrections, (TTC) for each station were computed for topography within a distance of 166.7 km of the station. This distance is equivalent to Hayford-Bowie zone "0" (Swick, 1942). A computer program written by D. L. Plouff (1977a) of the USGS which uses digital terrain data was used to compute terrain corrections. The program also incorporated a modification of the program developed by Plouff (1977b) which permitted the calculation of the terrain correction for the distance interval zero to 0.895 km, Hammer's zone F (Hammer, 1939). The digital terrain data was based on the National Cartographic and Information Center 0.01 inch digitization of 1:250,000 scale topographic maps. These data provide the average elevation in 0.5, 1.0 and 3.0 minute square areas. The gravitational effects of the topography were calculated for radial distances from zero to 2.29 km using topography digitized at 0.5 minute increments, from 2.29 km to 15 km using 1.0 minute data, and 15 km

to 166.7 km using 3 minute data. The terrain effect calculated for the area between 0 and 2.29 km of the station exceeded 5.0 mgls for 40 stations. Subsequently these stations were recalculated by hand, utilizing a method outlined by Oliver and others (1969).

Table 1 (Appendix) lists the principal facts for each gravity station in the Mount Hood study area. The table heading explains the column designations. The table does not list the parameters or values of special reductions or analyses described in this report, however, these can be calculated from the principal facts and the relations described in the appropriate text of this report.

Free-Air Gravity Anomalies

Figure 3 shows a free-air gravity anomaly map of the Mount Hood area based on measurements at the station locations shown in Figure 2. The map contours are at intervals of 10 mgl and heavy contours occur at 0, 50, 100 and 150 mgl levels. The free-air anomalies reflect the very irregular topography of the area and the 0 mgl contour of the gravity map coincides approximately with the 3000 foot topographic contour in Figure 1. The summit of Mount Hood, approximately in the center of the map, exhibits a free-air anomaly of greater than +150 mgls. Elongate gravity anomaly lows near $45^{\circ}30'N$ lat and $121^{\circ}35'$ and $121^{\circ}45'W$ long are oriented approximately north-south. The easternmost gravity anomaly low extends southward past Mount Hood at least to the southern limit of the survey area. The westernmost gravity low extends to just west of Mount Hood where it appears



FREE-AIR GRAVITY MAP
MOUNT HOOD AREA, OREGON



AREA OF THIS MAP

KILOMETERS

0 2 4 6 8

0 1 2 3 4 5

MILES

OREGON STATE UNIVERSITY

DECEMBER, 1977

GRAVITY DATA FROM
J THIRUVATHUKAL 1969 OSU
K KEELING 1977 OSU

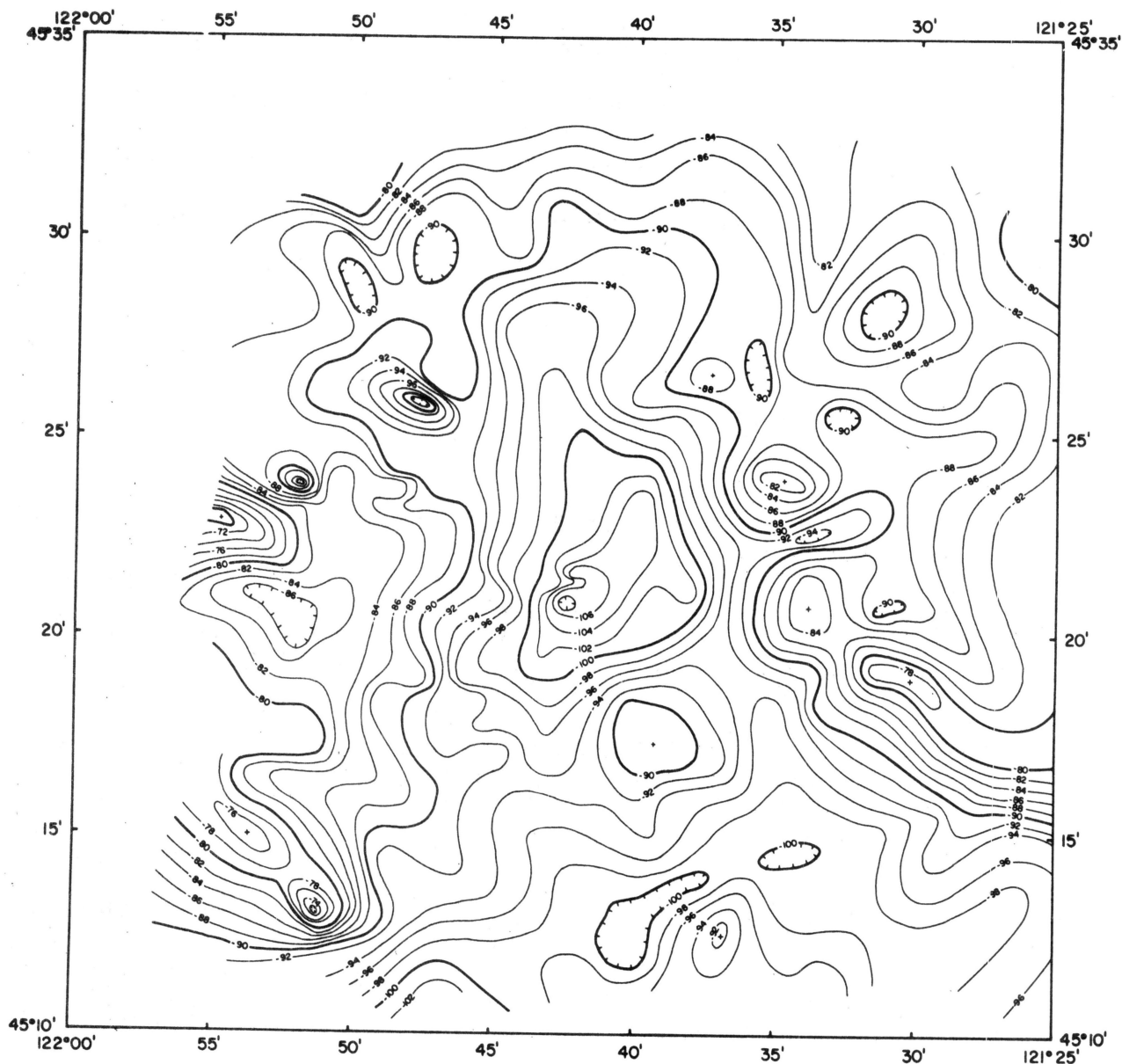
UNIVERSAL TRANSVERSE MERCATOR PROJECTION
CONTOUR INTERVAL 10 MGALS
ESTIMATED STATION UNCERTAINTY ±2 MGAL

Figure 3

to be interrupted by a series of gravity highs oriented approximately east-west. The two north-south trending lows suggest a major structural offset in the basement rocks beneath the post-Miocene rocks which form Mount Hood. The relatively short wavelength, positive anomalies associated with Mount Hood and the surrounding mountains suggest the mountains are not locally compensated to any significant extent and consequently are interpreted as localized loads imposed on a relatively rigid crust or lithosphere.

Bouguer Gravity Anomalies

Figure 4 shows a complete Bouguer gravity anomaly map of the Mount Hood area. The map, prepared using a standard reduction density of 2.67 gm/cm^3 , exhibits contours at intervals of 2 mgls and heavy contours at 10 mgl intervals. A marked gravity low of less than -108 mgls occurs on Mount Hood. This gravity low is the most negative part of a larger gravity low which extends north of Mount Hood to about $45^{\circ}30'$ and extends south of Mount Hood at least to the limit of the survey area. The negative anomaly, closed north of Mount Hood, is open to the south and suggests a large geologic feature on which Mount Hood is superimposed that begins in the vicinity of Mount Hood and extends southward. The anomalies east of Mount Hood near $45^{\circ}20-25' \text{ N lat}$ and $121^{\circ}30-34' \text{ W long}$ show only a small correlation with topography; hence, the average density of the near-surface rocks which form the topographic features is near 2.67 gm/cm^3 . The negative correlation between the topography and gravity anomaly of Mount Hood and the mountains west and south

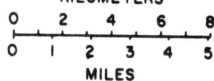


COMPLETE BOUGUER GRAVITY ANOMALY MAP
MOUNT HOOD AREA, OREGON



AREA OF THIS MAP

KILOMETERS



MILES

OREGON STATE UNIVERSITY
DECEMBER, 1978

GRAVITY DATA FROM
J. THIRUVATHUKAL 1969 O.S.U.
K. KEELING 1977 O.S.U.
G. NESS & J. BOWERS 1978 O.S.U.

UNIVERSAL TRANSVERSE MERCATOR PROJECTION
CONTOUR INTERVAL 2 MGALS
ESTIMATED STATION UNCERTAINTY ±2 MGAL
REDUCTION DENSITY 2.67 gm/cm³

Figure 4

of Mount Hood suggest the standard reduction density (2.67 gm/cm^3) is greater than the average density of the rocks which form the mountains.

Computation of the standard deviation of the complete Bouguer anomalies of a region yields an indication of the correlation of the anomalies and the topography of the region. Figure 5 shows a graph of the standard deviation of the complete Bouguer gravity anomaly as a function of density for the Mount Hood area. The curve shows a minimum when the density equals 2.27 gm/cm^3 . To determine a regional density for Mount Hood the gravity station data were separated into a set which included all the stations and a subset which included only the stations located on Mount Hood proper. Both sets of data indicate approximately the same density, 2.27 gm/cm^3 , when the standard deviation of the computed anomalies is a minimum. Although the density of 2.27 gm/cm^3 yields anomalies with a minimum correlation with the topography of the area, the curve in Figure 5 is relatively flat near the minimum and suggests the actual densities of the topographic features have a broad range. For example, the Bouguer gravity anomalies in Figure 4 suggest the average density of the mountains immediately east of Mount Hood is greater than 2.27 gm/cm^3 and may be as high as 2.7 gm/cm^3 .

Figure 6 shows a complete Bouguer anomaly map of the Mount Hood area based on a reduction density of 2.27 gm/cm^3 . The Bouguer anomaly associated with Mount Hood is less than -64 mgls ; however, it is actually an anomaly high with respect to the surrounding anomalies. The anomaly high associated with

STANDARD DEVIATION OF THE COMPLETE BOUGUER
ANOMALY AS A FUNCTION OF DENSITY
MT. HOOD, OREGON

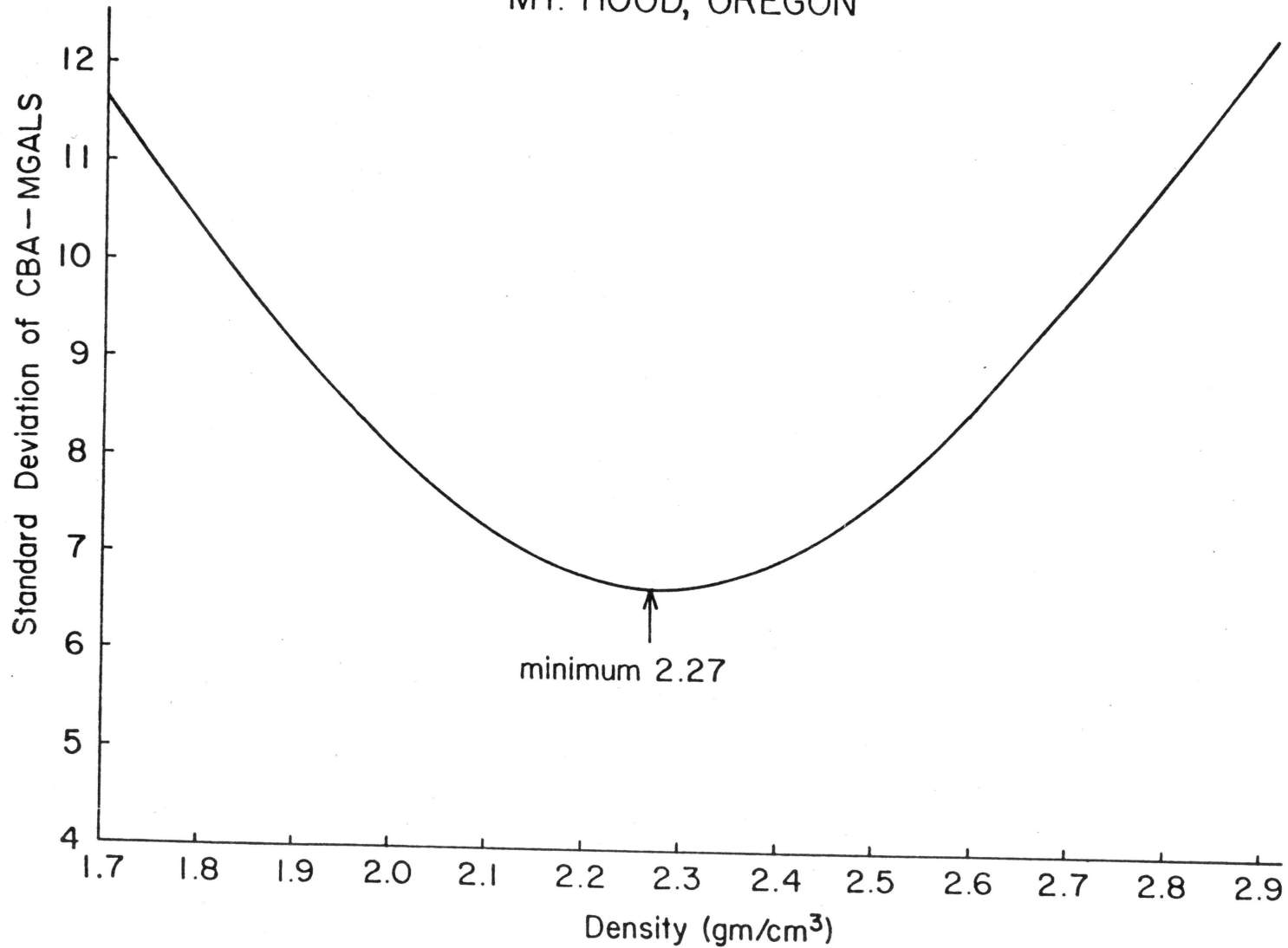
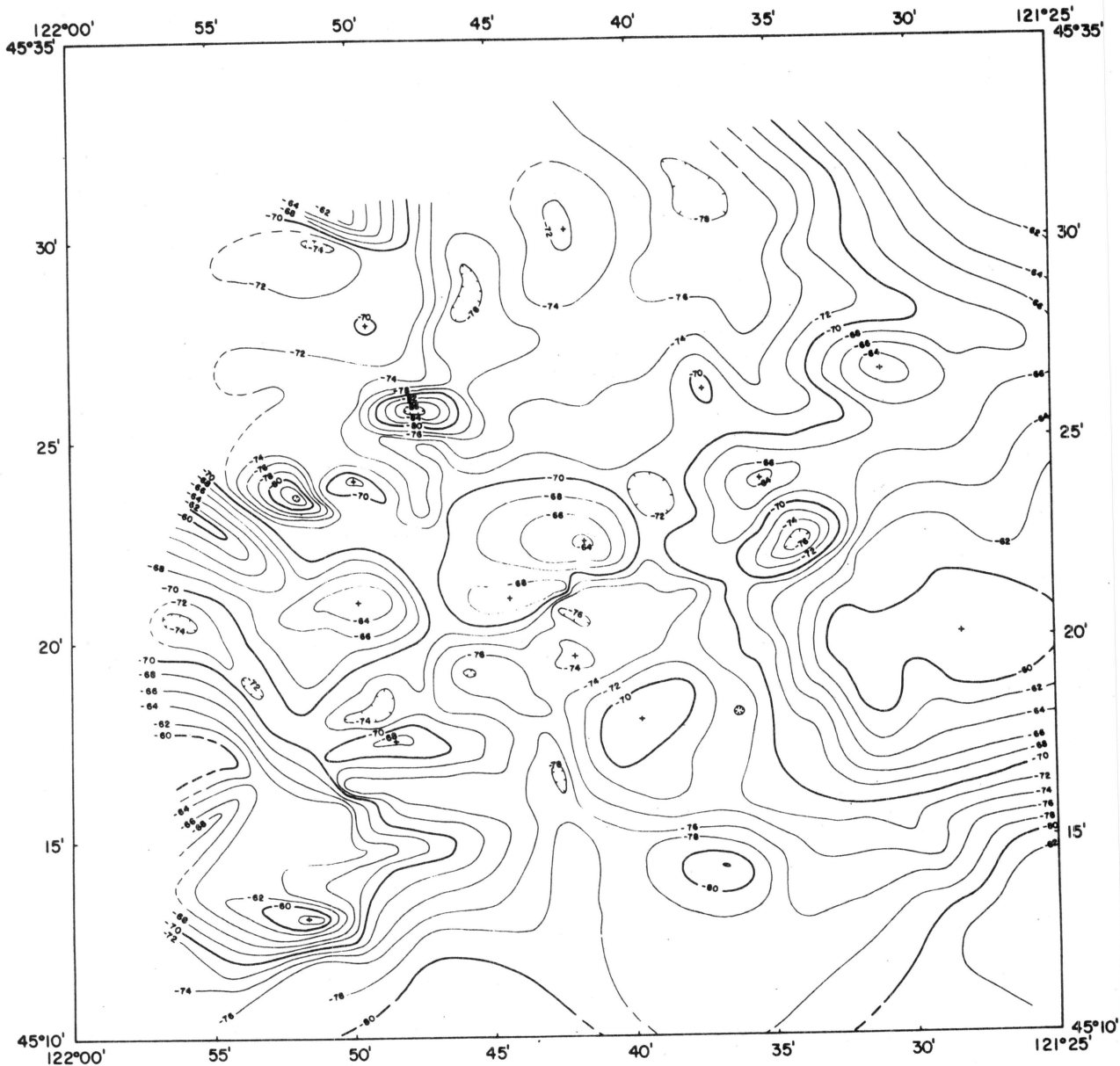


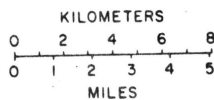
Figure 5



COMPLETE BOUGUER GRAVITY ANOMALY MAP
MOUNT HOOD AREA, OREGON



AREA OF THIS MAP



OREGON STATE UNIVERSITY
DECEMBER, 1978

GRAVITY DATA FROM
J. THIRUVATHUKAL 1969 OSU
K. KEELING 1977 OSU
G. NESS & J. BOWERS 1978 OSU

UNIVERSAL TRANSVERSE MERCATOR PROJECTION
CONTOUR INTERVAL 2 MGALS
ESTIMATED STATION UNCERTAINTY ±2 MGAL
REDUCTION DENSITY 2.27 gm/cm³

Figure 6

Mount Hood is flanked on the northeast and southwest by Bouguer anomaly highs. Together, these contiguous highs suggest a structural high, oriented approximately N75E, beneath the Plio-Pleistocene rocks which form Mount Hood and the surrounding mountains. The gravity high transects at an angle what appears to be an extensive north-south oriented gravity low. The east side of the gravity low exhibits higher gradients and is generally better delineated than the west side. The low suggests a graben-like structure with the east farther down and/or bounded by more prominent faults than the west side.

This interpretation of the gravity anomalies suggests Mount Hood sets in and covers to some extent a north-south oriented graben. The gravity high near the center of Mount Hood suggests its location may be structurally controlled in that the central vent lies along a structural ridge indicated by the contiguous gravity highs which cross the north-south gravity low. An alternative explanation of the gravity high associated with Mount Hood is that it reflects the internal structure of the mountain and may indicate the main vent or core of the mountain. Because of the sparcity of stations, gravity anomalies are not well delineated near the summit.

South of Mount Hood, near 45°15'N lat., gravity gradients suggest a structural lineation oriented approximately N85 E. The senior author has speculated, on the basis of the alignment of earthquake epicenters and SLAR imagery, that a fault - possibly a thrust fault - may extend along the base of Mount Hood on the south side. The gravity anomalies are consistent

with this hypothesis but do not strongly support it.

Prominent lineations in the gravity anomalies oriented approximately $N23^{\circ}W$ occur both northeast and southwest of Mount Hood. Two lineations northeast and two southeast of Mount Hood appear to extend completely across the area mapped in the gravity survey and may be complementary to the east northeast-south southwest lineations described above.

Many closed short-wavelength anomalies occur also in the area and are very likely associated with surface or very near surface structural and/or compositional features.

Closely spaced gravity stations occur along lines which extend north, south, east and west from gravity station GS 33 which is located 70 feet west of the geothermal drill hole south of Timberline Lodge. To obtain accurate gravity measurements differential leveling was used to determine the station elevations. The initial elevation, 5936', was stamped in the USDA, Bureau of Public Roads BM 50-1, located in the front steps of Timberline Lodge. A stadia survey connected all gravity stations to an X-Y coordinate system. The initial azimuth, 190° , was scaled from the Pucci chairlift as shown on 7.5 minute USGS Topographic Map, Mount Hood. Poor weather prevented additional ties. Longitudes and Latitudes of the stations were computed based on:

- a) The initial station MHL 8 latitude ($45^{\circ} 19.87'$) and longitude ($121^{\circ} 42.61'$)
- b) The scale 1" of latitude = 101.27 feet at $45^{\circ}20'$ N lat. as per Oregon Plane Coordinate Projection Tables SP 270

- c) And a scale ratio at $45^{\circ}20'$ of 1" long/1" lat =
0.708 and 1" long = 71.699 feet.

Table 1 in the back of this report lists the latitude, longitude and gravity anomaly values for the gravity survey near the Timberline drill site.

Figure 7a shows a complete Bouguer gravity anomaly, based on a reduction density of 2.67 gm/cm^3 , around the Timberline geothermal drill site at approximately $45^{\circ}19.7'N$ lat, $121^{\circ}42.6'W$ long. The map indicates a general east-west trend to the anomaly contours and decreasing anomalies towards the north away from the drill site. The gravity anomalies contoured at an interval of 2 mgls suggest a relatively uniform structure in the vicinity of the drill site and rock layers of a relatively low density.

Figure 7b shows a complete Bouguer anomaly of the same area as Figure 7a but based on a reduction density of 2.27 gm/cm^3 . This density as discussed previously, is more representative of the average density of the rocks of Mount Hood. Figure 7b indicates that the drill site is located on a relative gravity high. The Bouguer anomaly high is of low amplitude and closed. The anomaly suggests a thickening of the more dense layers which form this sector of Mount Hood, an intrusive body, or a doming of the layers. A density contrast of 0.6 gm/cm^3 between massive andesite (2.6 gm/cm^3) and andesitic ash containing water (2.0 gm/cm^3) suggests a flow or intrusive thickness of approximately 80 m. A relatively steep gradient in the gravity anomalies which trends approximately east north-east-west southwest occurs north of the drill site near $45^{\circ}21'N$

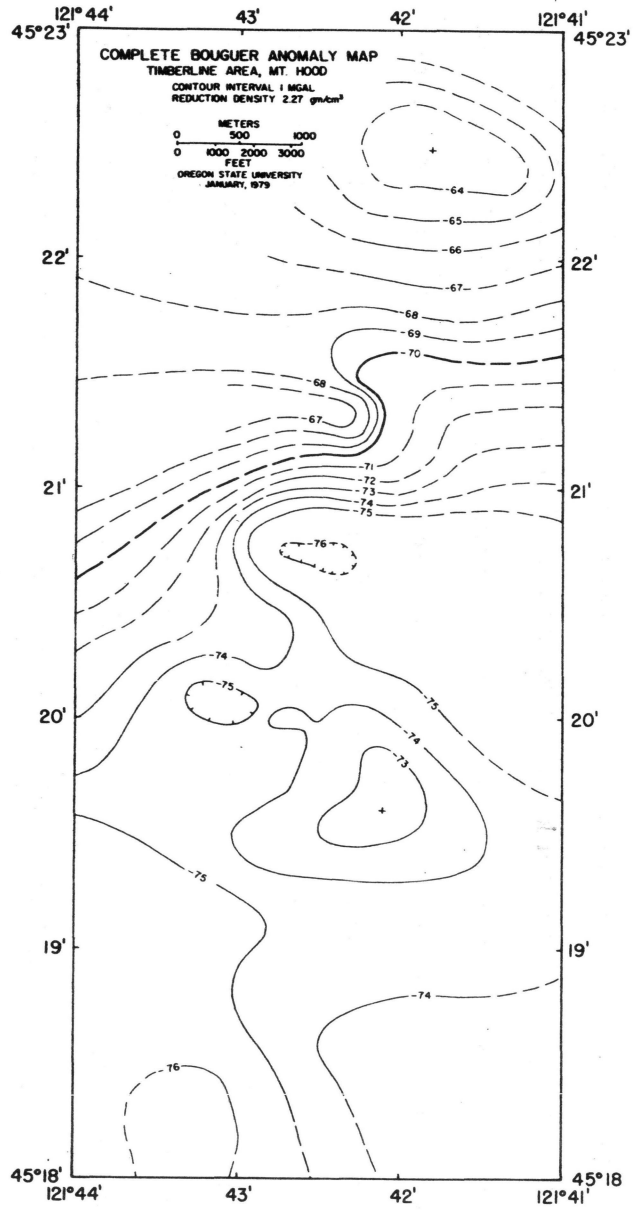


Figure 7b

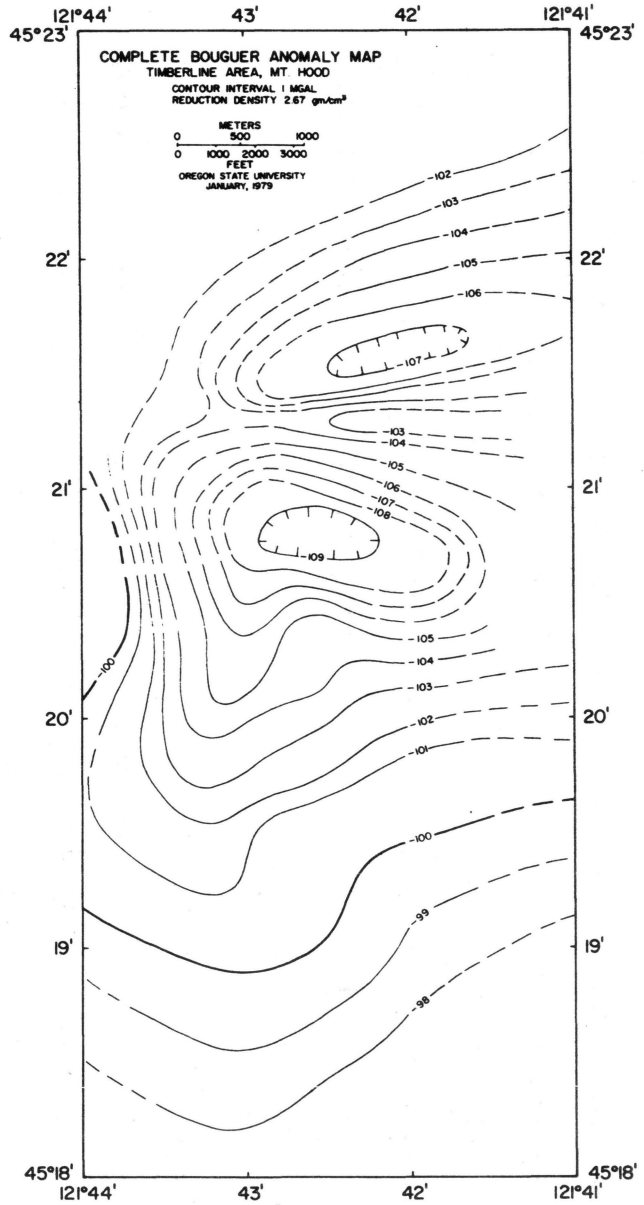


Figure 7a

lat. The anomaly is positive to the north and suggests that either a higher density layer (or flow) extends southward beneath the surface ash and cinder to approximately $45^{\circ}21'$ or that a structural break (or fault) occurs in the subsurface layers with the southside down about one mile north of the drill site. Other interpretations are also possible, however, the gravity measurements do not indicate any marked lateral variations in structure or density in the immediate vicinity of the drill site.

Regional Gravity Anomalies

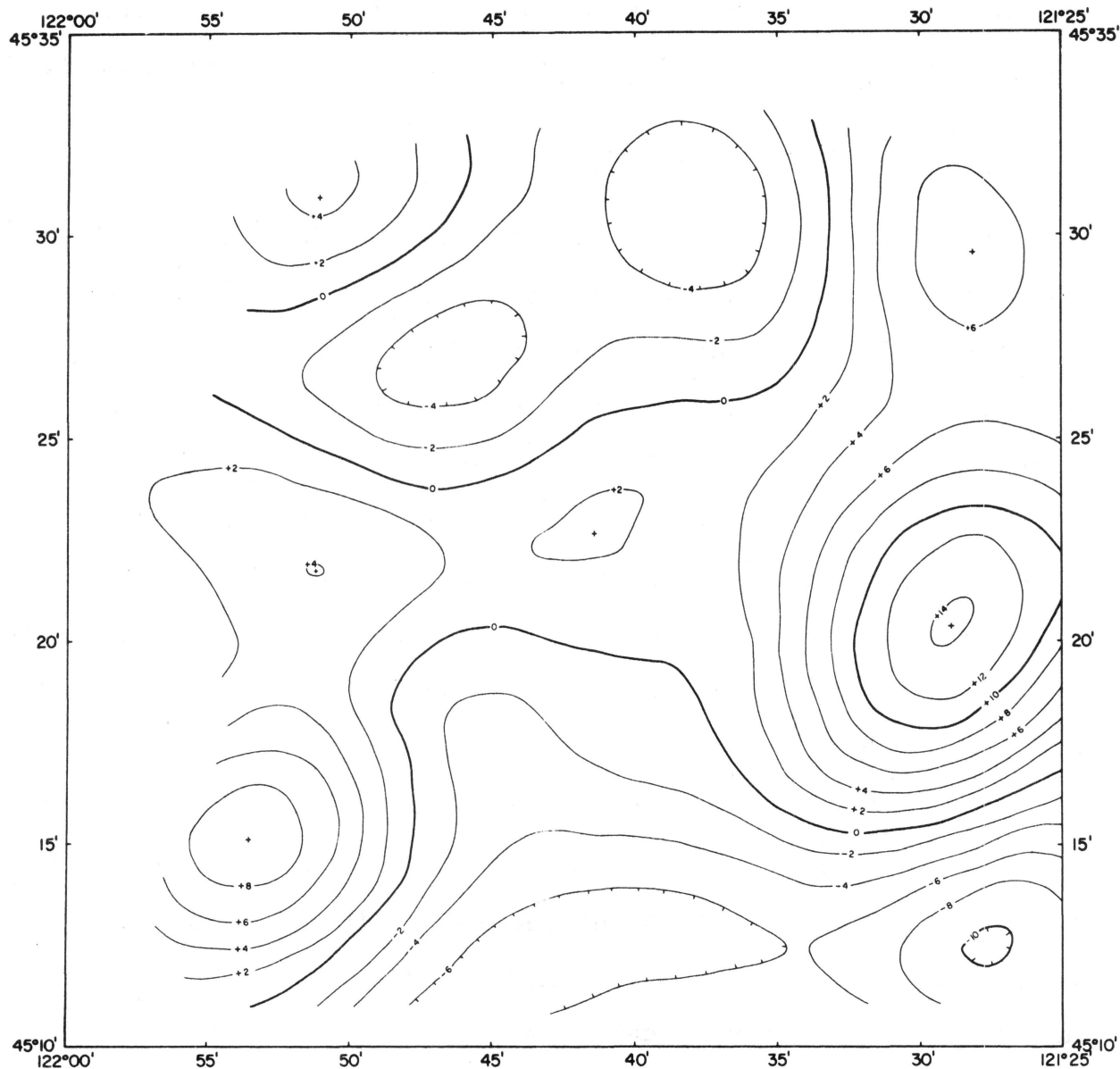
Spectral separation of the short and long wavelength components of the complete Bouguer anomalies of the Mount Hood area yields "regional gravity anomalies" and "residual gravity anomalies". Estimates of the frequency at which the spectral separation should occur were based initially on the wavelengths of the topography of the region. The authors postulated that, because of a relatively high density contrast, the long wavelength gravity anomalies more likely would be associated with the pre-Pliocene rocks of the region such as the Columbia River Basalts and the short wavelength anomalies would reflect shallow sources caused by lateral and vertical variations in the Pliocene and Holocene rock and ash which form Mount Hood and the surrounding mountains of the High Cascades. The initial spatial frequency separating the long and short wavelength parts of the gravity anomaly spectrum was 5 cycles per 65 kilometers or 13 km per cycle. Later iterations based on attempts to determine a "surface" for the Columbia River Basalts from the gravity

measurements as described below indicated a better separation of the anomaly wavelengths occurred at 8 cycles per 65 km or 8.1 km/cycle. Subsequently regional and residual anomalies separated spectrally at 8.1 km/cycle, were recomputed from the complete Bouguer anomalies shown in Figure 6.

Figure 8 shows a map of the regional gravity anomaly of the Mount Hood area with wavelengths longer than 13 km. The map shows gravity highs which trend generally north-south on the east and west sides of the map. Between the gravity highs a north-south trending gravity low suggests a depression or graben-like structure in the upper crustal rocks beneath the post-Miocene rocks of the High Cascades. A gravity high oriented approximately east-west transects the large north-south gravity low. The center of Mount Hood is located approximately on the east-west gravity high and the mountain's "core" may contribute to the positive anomaly.

Figure 9 shows a map of the residual gravity anomalies of the Mount Hood area shorter than 13 km. The map shows a large number of closed gravity highs and lows. These anomalies suggest density variations in the post-Miocene rocks of the area and may relate to individual flows or intrusions. No attempt was made to correlate these anomalies with the surface or near-surface geology.

Figure 10 shows a map of the regional gravity anomaly of the Mount Hood area with wavelengths longer than 8.1 km. The map includes shorter wavelength components than the map shown in Figure 8 and therefore shows more irregularity or character in the anomaly contours and steeper anomaly gradients.

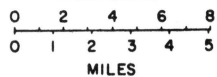


REGIONAL GRAVITY MAP
MOUNT HOOD AREA, OREGON

CONTOUR INTERVAL 2 MGALS



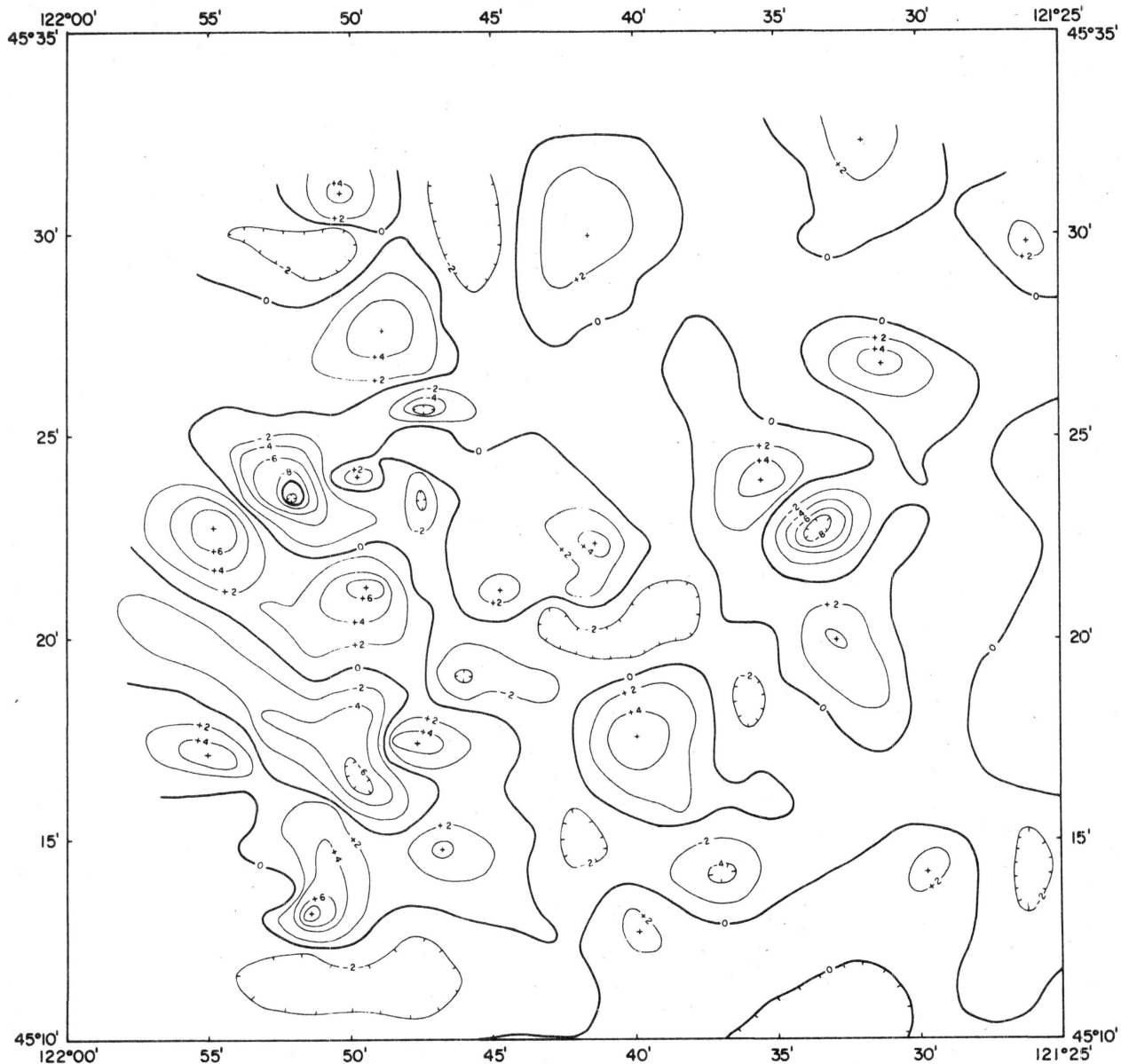
AREA OF THIS MAP
KILOMETERS



UNIVERSAL TRANSVERSE MERCATOR PROJECTION

OREGON STATE UNIVERSITY
DECEMBER, 1978

Figure 8

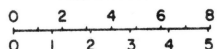


RESIDUAL GRAVITY MAP
MOUNT HOOD AREA, OREGON



AREA OF THIS MAP

KILOMETERS



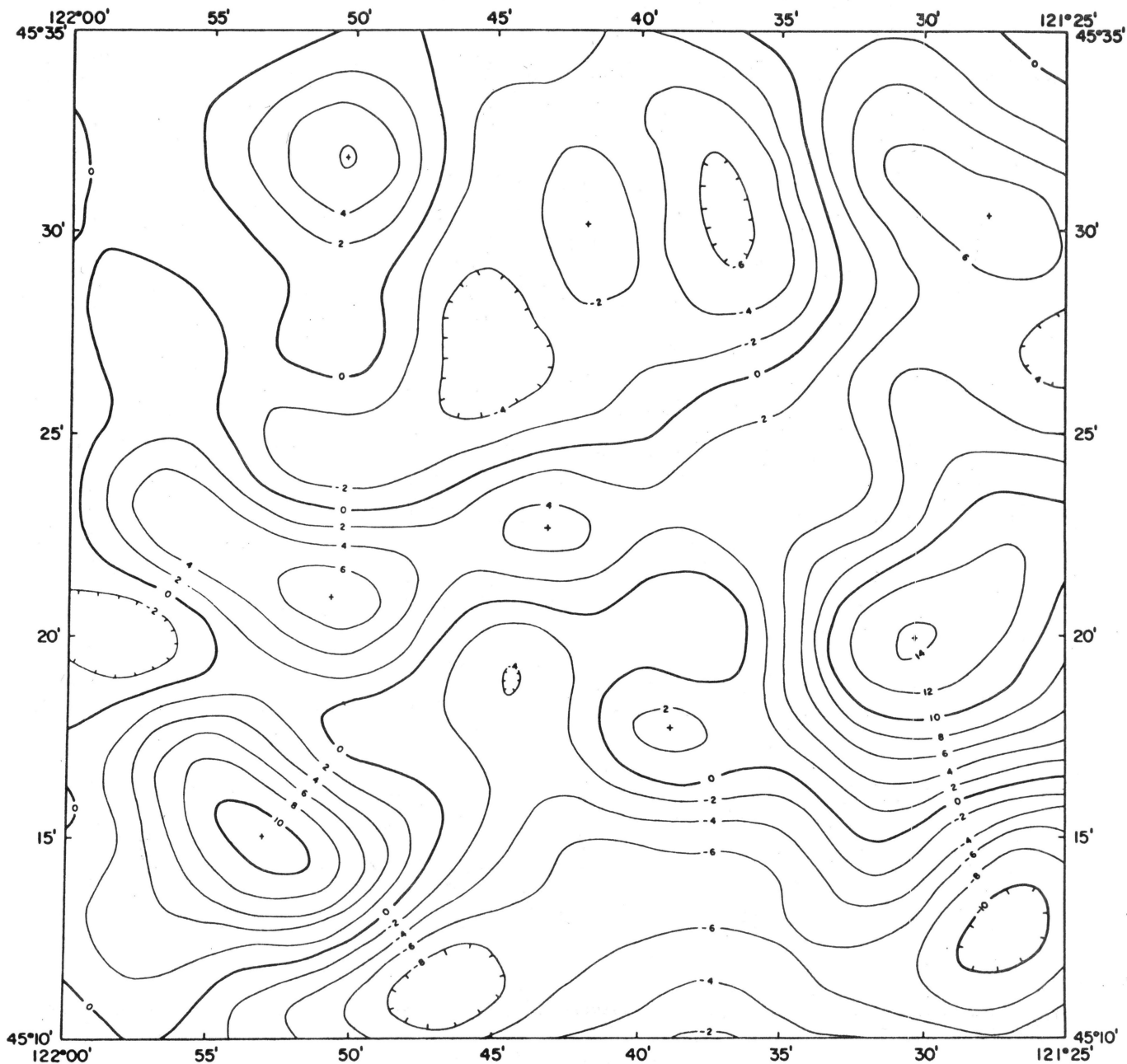
MILES

OREGON STATE UNIVERSITY
DECEMBER, 1978

CONTOUR INTERVAL 2 MGALS

UNIVERSAL TRANSVERSE MERCATOR PROJECTION

Figure 9

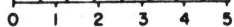


REGIONAL GRAVITY ANOMALY MAP
MOUNT HOOD AREA, OREGON



AREA OF THIS MAP

KILOMETERS



MILES

OREGON STATE UNIVERSITY

FEBRUARY, 1979

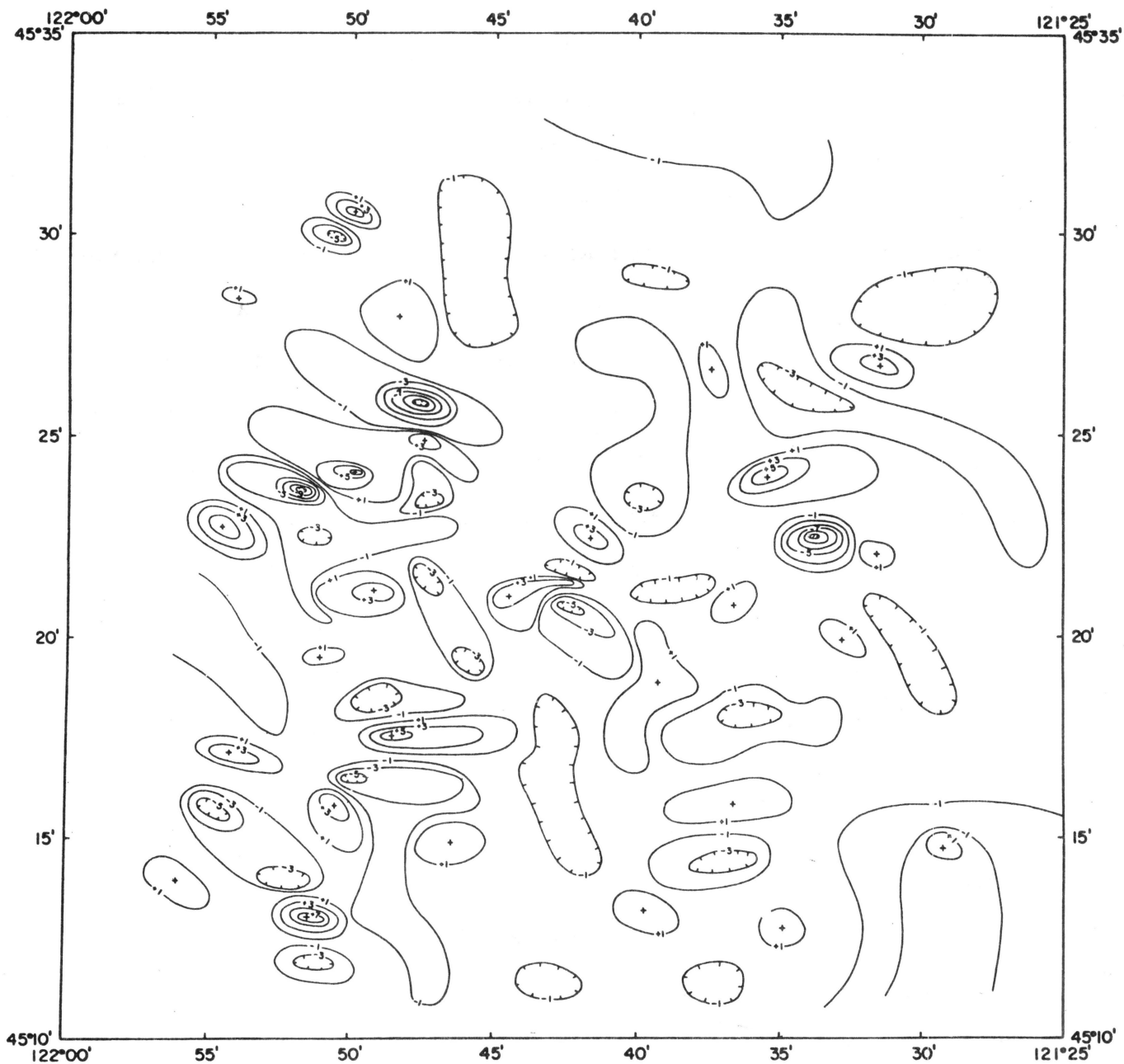
CONTOUR INTERVAL 2 MGALS

UNIVERSAL TRANSVERSE MERCATOR PROJECTION

Figure 10

Contiguous gravity highs, aligned north and south, occur east and northeast as well as west and southwest of Mount Hood. These highs together with a high northwest of Mount Hood flank a north-south oriented low. A relatively narrow high oriented approximately N75E, connects the highs on the western side with the highs on the eastern side and suggests a linear structure or an offset in structure beneath Mount Hood. A gravity low, south of Mount Hood, approximately parallels the N75E gravity high and intersects or truncates the north-south oriented highs east and west of Mount Hood. Hence two dominant anomaly lineations are evident; approximately north-south and approximately N75E. The north-south lineations suggest a graben-like structure in which Mount Hood is located and the east-northeast lineations that suggest folds and/or faults which cross the graben-like structure. The anomalies are relatively long wavelengths and are likely associated with the more dense pre-Pliocene rocks beneath Mount Hood and the surrounding mountains.

Figure 11 shows a map of the residual gravity anomalies of the Mount Hood area shorter than 8.1 km. The map shows a large number of closed gravity highs and lows of small areal extent. These anomalies suggest local density variations in the post-Miocene rocks of the area and may relate to individual flows or intrusions or relatively thick ash deposits. The station location density and the smoothing inherent in the computations and subsequent contouring of the data limit the resolution of the individual anomalies and consequently the anomaly causing bodies. No attempt was made to correlate

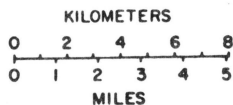


RESIDUAL GRAVITY ANOMALY MAP
MOUNT HOOD AREA, OREGON



AREA OF THIS MAP

CONTOUR INTERVAL 2 MGALS



UNIVERSAL TRANSVERSE MERCATOR PROJECTION

OREGON STATE UNIVERSITY
FEBRUARY, 1979

Figure 11

these anomalies with the surface or near-surface geology.

MODELS OF MOUNT HOOD

A large number of geological, geophysical, and geochemical studies contemporary with the gravity study described in this report will provide data with which to constrain future models of the internal and substructure of Mount Hood. Simple models, based on only a few gravity values, are offered and described below which may suggest limits or directions to other investigators studying Mount Hood. Topographic elevations, a Bouguer gravity anomaly based on a measurement on the summit of Mount Hood of 7.6 mgls, and an anomaly wavelength based on gravity measurements on the flanks of Mount Hood constrain the simple models.

Figure 12 shows a sphere model of Mount Hood that agrees with the observed Bouguer gravity anomaly and anomaly wavelength. The model assumes a density contrast, $\Delta \rho$, of 0.6 gm/cm³ between mountain and "core". Because the average density associated with the topography of the region is approximately 2.3 gm/cm³ the density of the spherical core would be approximately 2.9 gm/cm³. A density of 2.9 gm/cm³ would be near the maximum density expected for a volcanic core particularly if it were warm, altered and/or fractured. The size of core required to satisfy the observations and assumptions suggests the model is unrealistic.

Figure 13 shows a graph of a family of curves which describe the height and radius of a cylindrical core which satisfies the observed gravity anomaly on the summit of Mount Hood. The heavy curve which crosses the family of curves of different

SPHERE MODEL FOR MT. HOOD

Based on Peak Gravity Anomaly
and Anomaly Half-Width

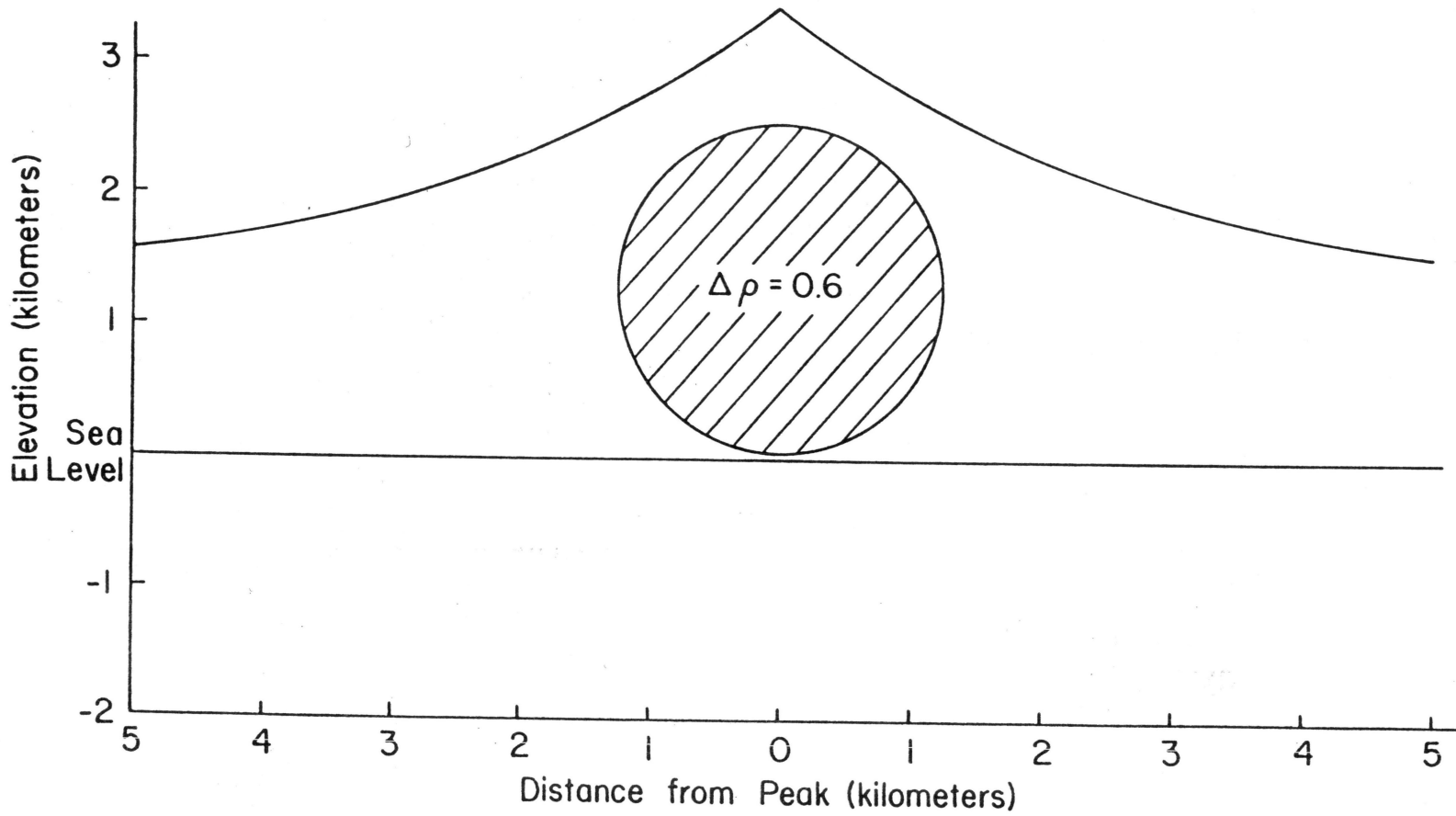
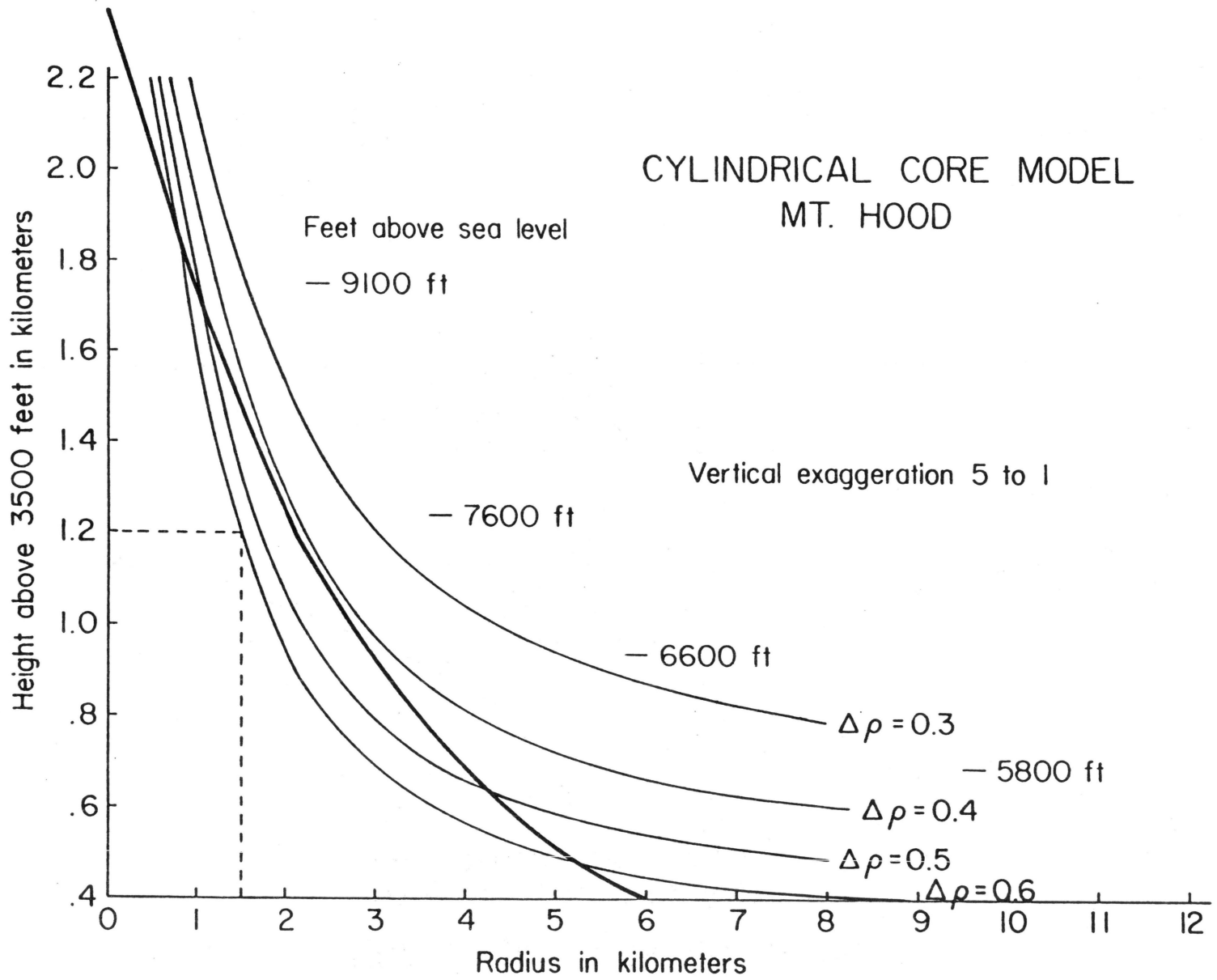


Figure 12

Figure 13



density contrasts is the smoothed topography of Mount Hood; therefore, any cylindrical model postulated is limited in radius and/or height by the topography. The dotted line illustrates one possible model: the cylinder has a radius of 1.5 km, a height of 1.2 km (above an assumed base for Mount Hood of 3500 ft), and a density contrast of 0.6 gm/cm^3 . Smaller density contrasts yield larger cylinders but the minimum density contrast, limited by the topography, is slightly greater than 0.4 gm/cm^3 .

Figure 14 shows a cylinder plus cone model of Mount Hood which satisfies the observed gravity anomaly, and topography. This model implies that the higher density rock of the volcanic core extends to the surface at the summit of the mountain. This is consistent with the resistant rocks which are visible near the summit and which are probably more dense than most of the rock on the flanks of the mountain. Figure 12 illustrates the size of the core when a density contrast of 0.5 gm/cm^3 is assumed. In this model the base of the cylindrical core rests on Columbia River Basalt at an elevation of 3500 ft; however, it could extend much deeper without significantly altering the gravitational effect of the model. Changes in the dimensions of the model near the summit cause the larger changes in the gravitational attraction of the cylinder and cone model. Figure 15 shows a graph of the changes in radius of the cylinder and core models versus the density contrast between the cylinder and core and the surrounding mountain. The curve assumes the density of the surrounding rock is 2.27 gm/cm^3 and the observed Complete Bouguer anomaly is 7.6 mgls. A large

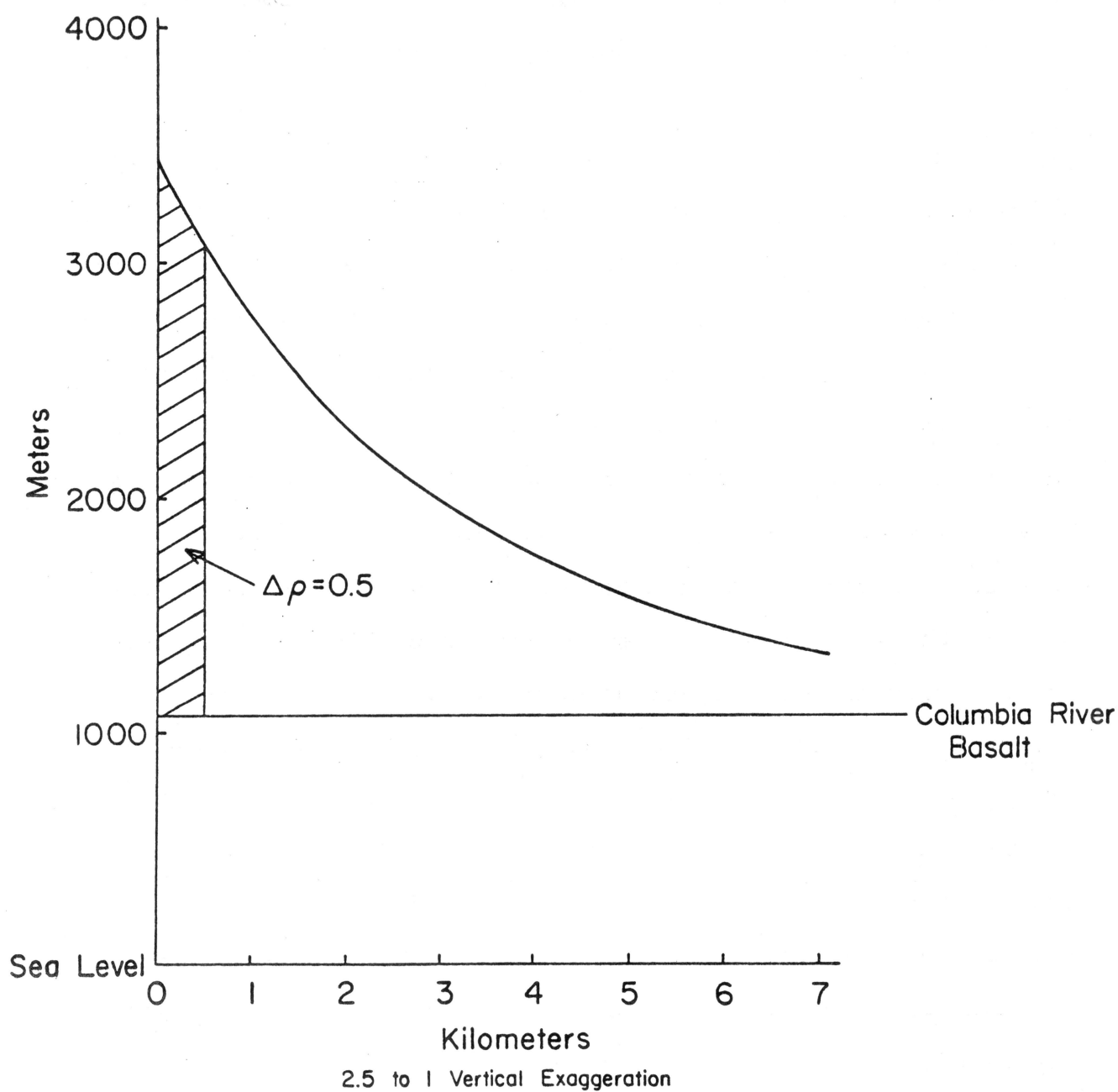
CYLINDER AND CONE MODEL FOR
CENTER OF MT. HOOD

Figure 14

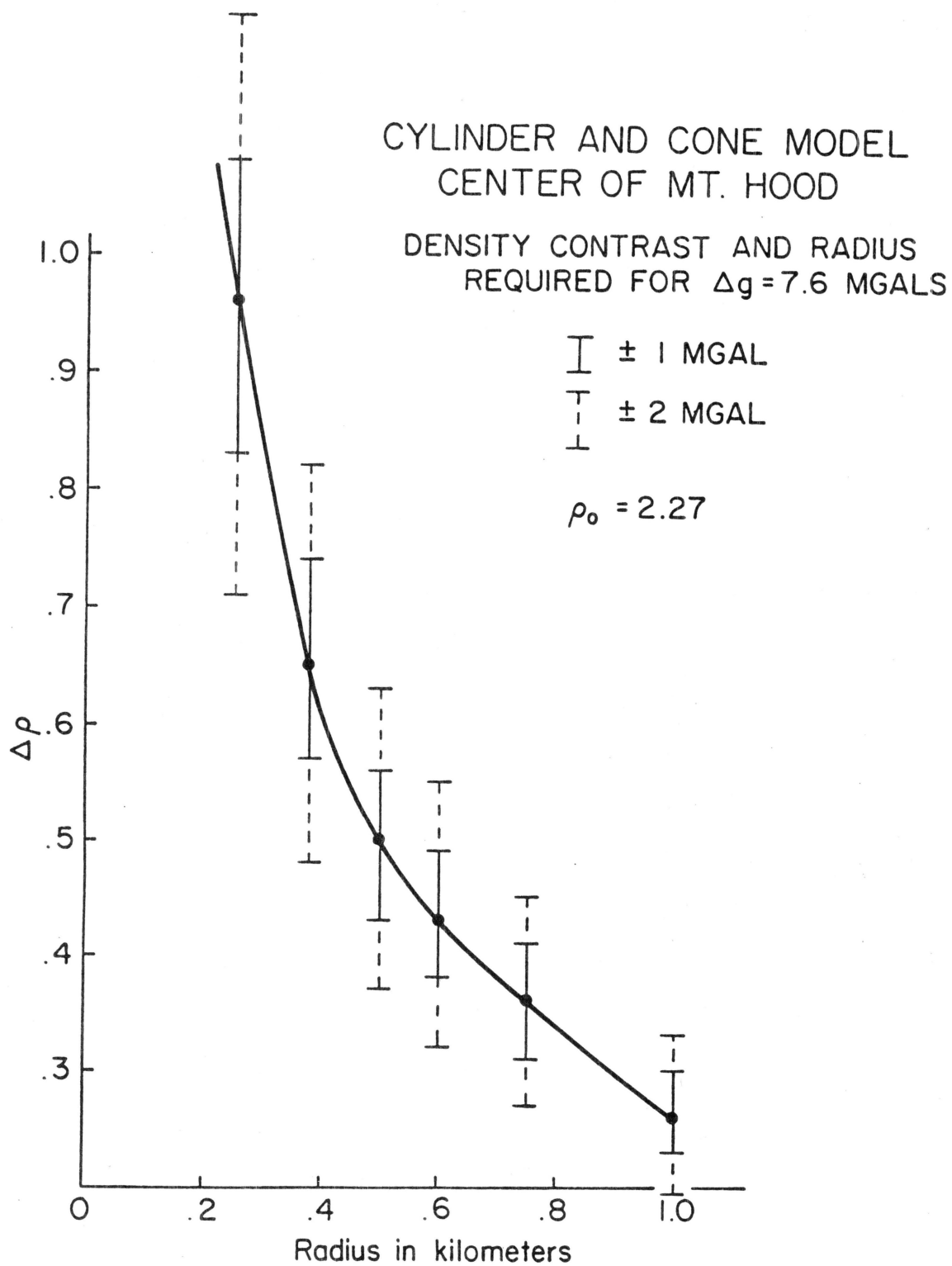


Figure 15

uncertainty is associated with the terrain correction of the summit anomaly on Mount Hood; hence, error bars of \pm and ± 2 mgls are shown on the curve to indicate the uncertainties in the resulting models.

ELEVATION OF THE COLUMBIA RIVER BASALT

The 2.27 gm/cm^3 density of the rocks which form the topography of and about Mount Hood is considerably less dense than the density of 2.7 to 2.9 gm/cm^3 generally associated with the Columbia River Basalts. Therefore, the gravity anomalies of the area contain information on the structure or the shape of the interface between the Columbia River Basalts and the overlying rocks. To estimate the elevation of the Columbia River Basalt (Yakima Basalt) the complete Bouguer gravity anomalies, computed with a reduction density of 2.27 gm/cm^3 , were spectrally separated into regional and residual components. The regional components that represent the anomaly field caused by the Columbia River Basalts were determined, after several interactions, to be best approximated by anomaly wavelengths longer than 8.1 km . The geologic map of the area indicates the Columbia River Basalts outcrop in several areas about Mount Hood. The elevations of the outcrops and the corresponding gravity anomalies provide a reference point for computations of the elevation of the Columbia River Basalt. The reference point selected was an elevation of 1040 meters and a gravity anomaly of $+4 \text{ mgls}$. The equation to compute the elevation at other gravity stations was then

$$H = \left(\frac{\text{RCBA}_{2.27}^{-4}}{41.92 \Delta \rho} \right) 1000 + 1040$$

where

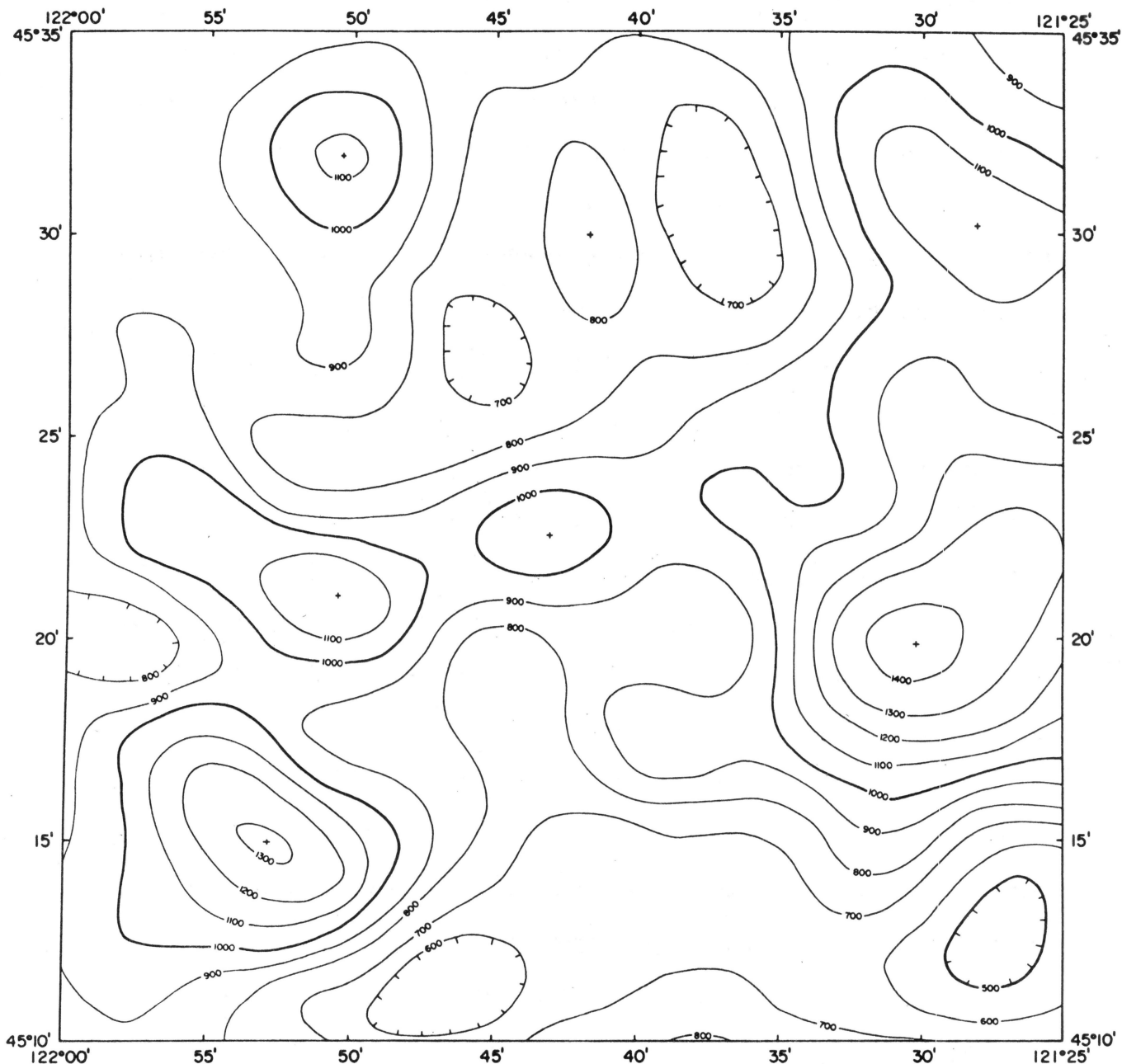
H = is the elevation in meters of the Columbia River Basalt above sea level

$\text{RCBA}_{2.27}$ = is the complete regional Bouguer anomaly at a reduction density of 2.27 gm/cm^3

= is the assumed density contrast between the Columbia River Basalt and the overlying flows and pyroclastics.

Elevations were computed for density contrasts of 0.4 and 0.6 gm/cm³. A density contrast of 0.6 gm/cm³ yields the best fit to the mapped outcrops of the Columbia River Basalt. Figure 16 shows the estimated elevations of the top of the Columbia River Basalt (Yakima Basalt) based on computations that used a regional gravity field with spatial anomaly wavelengths greater than 8.1 km. The contour interval is 100 m with heavy contours shown at an elevation of 1000 m. Undulations in the surface range from less than 500 to greater than 1400 m above sea level. The highest elevations occur on the east, north-east and southwest sides of Mount Hood. The axis of Mount Hood is located approximately on an elevated ridge, oriented approximately N75E, that extends from the high elevations of the Columbia River Basalts on the east side of Mount Hood to the high on the southwest side.

Elevation estimates of the Columbia River Basalt is based on gravity measurements, an assumed density contrast between the Columbia River Basalts and the post-Miocene pyroclastics and flows of the High Cascade Mountains, and a reference elevation and gravity anomaly on an outcrop of the Columbia River Basalts in the study area. Inherent in these estimates are limits on the resolution of the surface configuration and elevation imposed by the position and spacing of the primary data grid and the continuity or smoothness of potential fields. Further, the elevations are computed independently for each station. Because of the limitations inherent in the method of

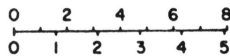


ESTIMATED ELEVATION OF THE COLUMBIA RIVER BASALTS
MOUNT HOOD AREA, OREGON



AREA OF THIS MAP

KILOMETERS



MILES

OREGON STATE UNIVERSITY
FEBRUARY, 1979

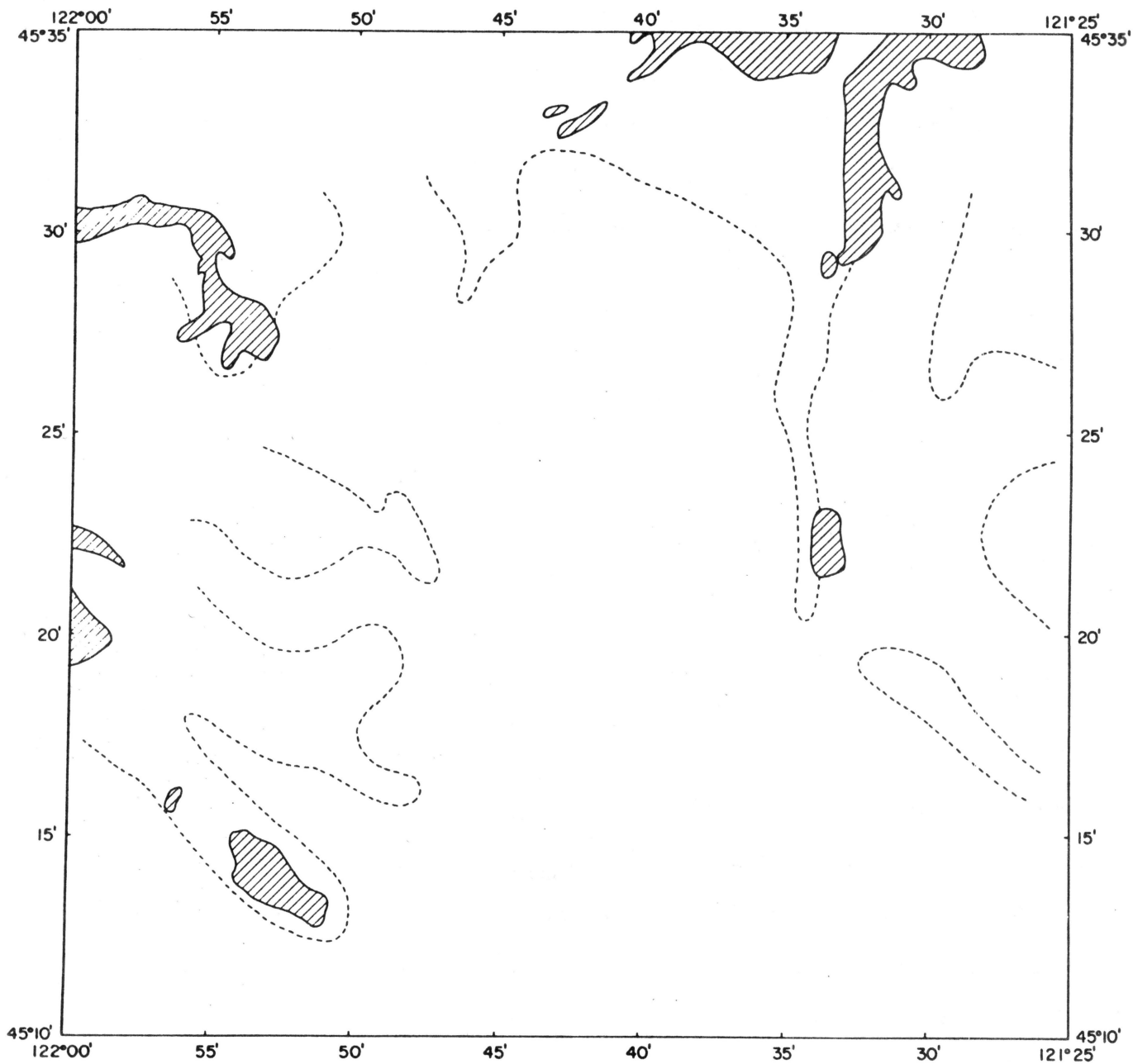
CONTOUR INTERVAL 100 METERS

UNIVERSAL TRANSVERSE MERCATOR PROJECTION

Figure 16

estimating the elevations many features cannot be resolved. For example, features with edges, such as faults or lava flows, are smoothed and included in the undulations of the estimated topography. The method also cannot differentiate between flows or changes in the Columbia River Basalt and other high density flows in the area, hence their surface is mapped as Columbia River Basalt. High density intrusions in the material above the Columbia River Basalt may be reflected or included in the undulations of the basalt.

To assess the effectiveness of the elevation estimates the computed elevations were compared to topographic elevations to generate a map of the "computed outcrops" of the Columbia River Basalts. Figure 17 shows a map of both the observed and computed outcrops of the Columbia River Basalts. The agreement between computation and observation is reasonable but generally more Columbia River Basalt is expected to outcrop than is actually observed. This discrepancy may be caused by a wrong reference elevation for the computations, erosion of the basalt in the area of expected outcrops, insufficient geologic mapping, or broadening of the surface during computation and contouring. West of Mount Hood relatively high density rocks are associated with Pliocene volcanism.

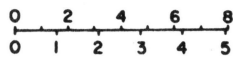


TOPOGRAPHIC SURFACE OF PRE-PLIOCENE ROCKS
MOUNT HOOD AREA, OREGON



AREA OF THIS MAP

KILOMETERS



MILES

OREGON STATE UNIVERSITY
FEBRUARY, 1979

COLUMBIA RIVER BASALT
OBSERVED OUTCROP 
COMPUTED OUTCROP 

UNIVERSAL TRANSVERSE MERCATOR PROJECTION

Figure 17

POROSITY ESTIMATES

Laboratory measurements on rocks from Mount Hood by Dr. N. Christianson (University of Washington, personal communication, 1978) show porosities of 6 to 7 percent in samples of fresh massive andesite. The measured samples have densities and p-wave velocities listed in Table 2.

TABLE 2

Sample	Density (gm/cm ³)	Velocity (km/sec)
1	2.56	4.49
2	2.58	4.52
3	2.60	4.65
4	2.62	4.52
5	2.62	4.97
6	2.59	4.84

The average density of the samples is 2.60 gm/cm³ and the average velocity is 4.67 km/sec. If $p_{2.6}$ is the density of andesite at 7 percent porosity, then p_{\max} , the density at 0 percent porosity is 2.80 gm/cm³. Recognizing that the rocks which form Mount Hood are believed to be more than 90 percent andesite (Wise, 1969) the value, p_{\max} , provides a reference point to compute average porosities for the rocks of Mount Hood above the Columbia River Basalts. The elevation difference, h , between the estimated elevation of the Columbia River Basalt and the topographic surface, the residual gravity anomalies (RGA), obtained as the difference between the complete Bouguer anomalies and the regional anomalies and the reduction density $p_{2.27}$, provide the parameters used to compute an average density

for the mass column between the Columbia River Basalts and the topographic surface. The equation is,

$$P_{avg} = P_{2.27} + \frac{RGA}{2\pi\sigma h}$$

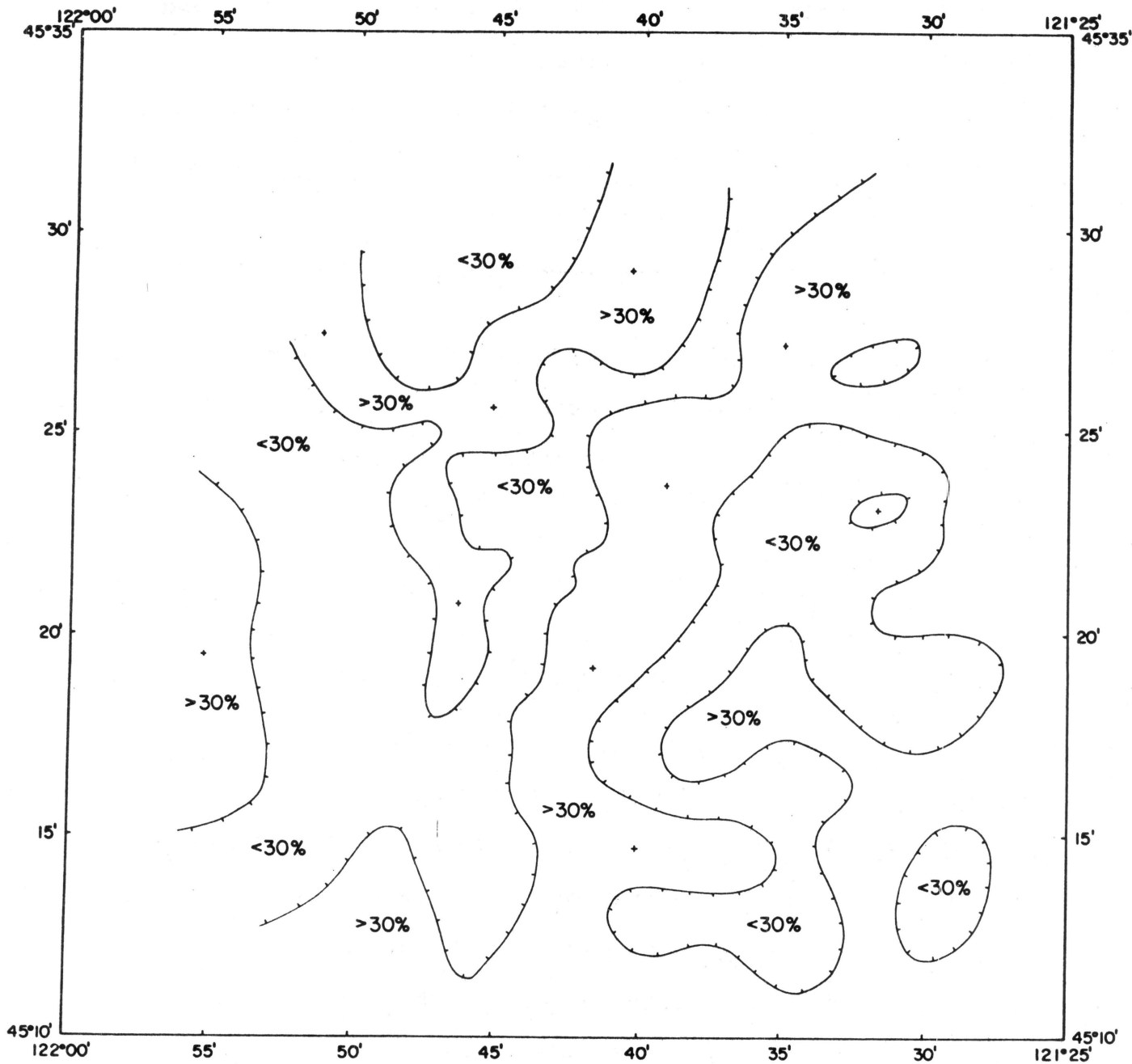
where σ is the gravitational constant. The estimated porosity is given by the equation:

$$\text{Porosity (\%)} = 100 \left(\frac{2.8 - P_{avg}}{2.8} \right)$$

Because the rocks are porous they can contain water, consequently the equation above yields a porosity for dry rocks. The equation for 100 percent water saturated rocks is:

$$\text{Porosity (\%)} = 100 \left(\frac{2.8 - P_{avg}}{1.8} \right)$$

Figure 18 shows a map of the estimated average porosities of the rocks in the Mount Hood area above the Columbia River Basalts based on the assumption that the rocks are water saturated. Because the computed values have large inherent uncertainties and show a large scatter or range in values they result in numerous "one-point" anomalies. Consequently, the computed values were smoothed and the contours only separate areas of porosities greater than or less than the average porosity, 30 percent, of water saturated rocks. The map shows an area east of Mount Hood with porosities less than 30 percent that corresponds reasonably well to the area where the complete Bouguer anomalies suggest the presence of higher density rocks. These observations of course, are not independent. A contour line that separates porosities of greater than 30 percent on the east side from porosities of less than 30 percent on the west side crosses the summit of Mount Hood from approximately south southwest to north northeast. The difference in the

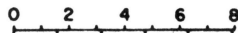


ESTIMATED REGIONAL POROSITY
MOUNT HOOD AREA, OREGON



AREA OF THIS MAP

KILOMETERS



MILES

OREGON STATE UNIVERSITY

FEBRUARY, 1979

UNIVERSAL TRANSVERSE MERCATOR PROJECTION

Figure 18

porosities indicated by the map suggests an asymmetry in the average rock, a composite of flows and pyroclastics, that forms Mount Hood. Alternatively, the average porosity of the rock materials may be the same about the summit and flanks of Mount Hood but the porous rocks may contain more water on the west side than on the east side.

TRAVEL TIME RESIDUALS

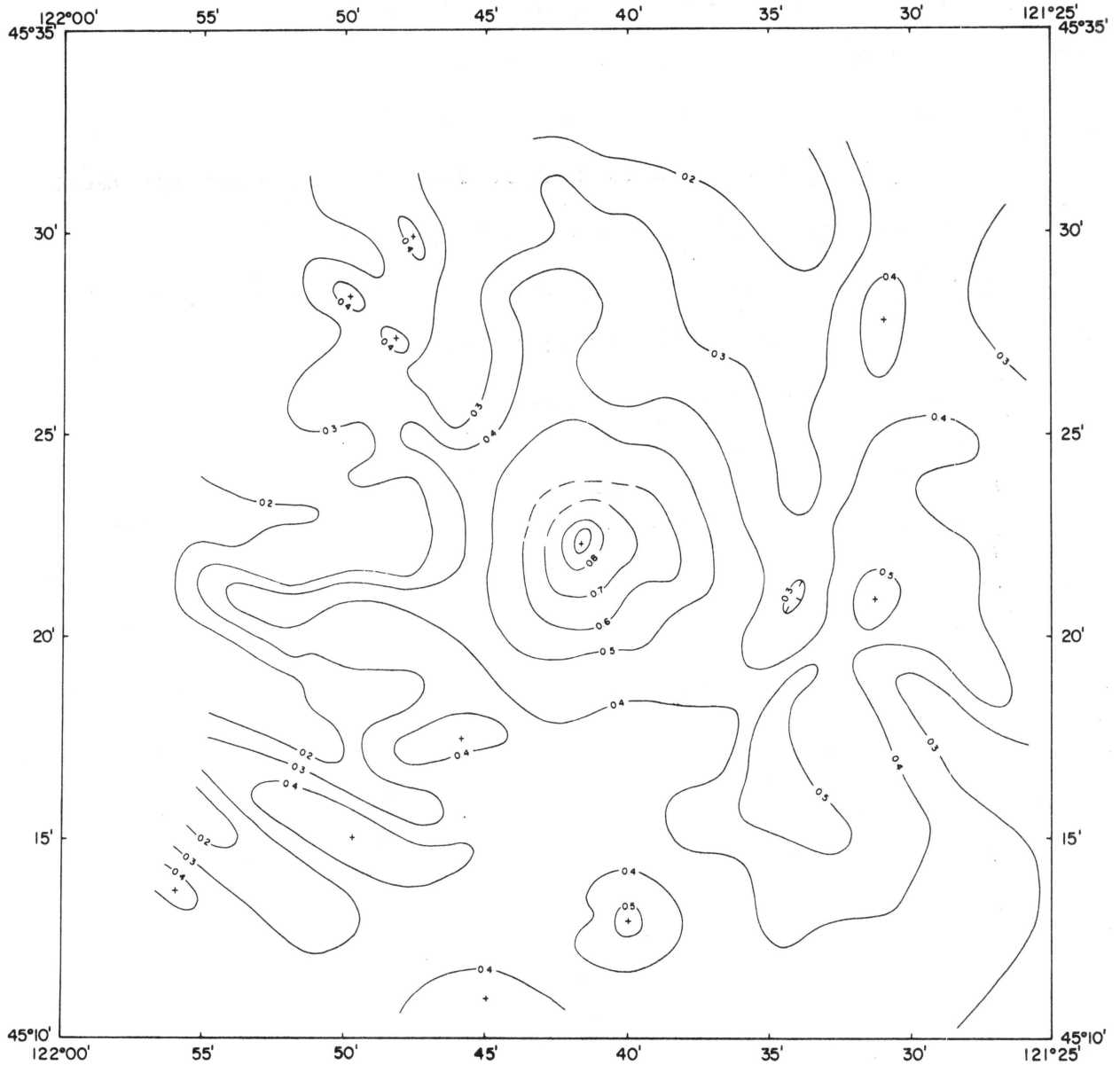
Empirical relations between rock density and compressional wave velocity (Ludwig, Nafe, and Drake, 1970) provide a means to estimate p-wave travel time residuals for the Mount Hood area based on gravity measurements. The empirical curves of Ludwig and others (1970) indicate a compressional wave velocity of approximately 3.3 km/sec for rock of density 2.27 gm/cm³. Recognizing that the average complete Bouguer anomaly for the Mount Hood area is -71.7 mgl then the approximate travel time vertically through the material above sea level is given by the equation:

$$\Delta T = \frac{h}{1.45 (2.27 + \Delta \rho)}$$

where h is the elevation in kilometers and

$$\Delta \rho = \frac{CBA + 71.7}{2 \pi \gamma h}$$

Figure 19 shows estimated travel time residuals for the Mount Hood area. The travel time residuals are the time of travel from sea level to the surface and the differences are caused by variations in topographic elevation and rock density along the ray path. The computed travel time residuals are estimates only and do not allow for irregular travel paths caused by refraction and diffraction of the seismic waves. The map does indicate, however, that significant travel time differences caused by near-surface effects can be expected.

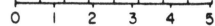
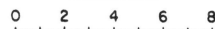


ESTIMATED TRAVEL-TIME RESIDUALS
MOUNT HOOD AREA, OREGON



AREA OF THIS MAP

KILOMETERS



MILES

OREGON STATE UNIVERSITY
JANUARY, 1979

CONTOUR INTERVAL 0.1 SEC

UNIVERSAL TRANSVERSE MERCATOR PROJECTION

Figure 19

ACKNOWLEDGEMENTS

Messuers. K. Keeling, T. Jones, W. Plant, G. Ness, M. Brown, and J. Bowers made the gravity measurements in the Mount Hood area. S. Pitts, K. Keeling, D. Braman, J. Cook, G. Axelsson and W. Avera assisted in the data reduction. P. Pitts, B. Priest, D. Burt, and S. Troseth prepared the maps and illustrations, J. Brenneman and N. Kneisel helped prepare the report. This work was supported by the Oregon State Department of Geology and Mineral Industries through a grant from the U. S. Department of Energy.

REFERENCES

- Hammer, Sigmond, 1939, Terrain Corrections for Gravimeter Stations, *Geophysics*, v. 4, p. 184-194.
- Longman, I. M., 1959, Formulas for computing the tidal accelerations due to the moon and the sun: *J. of Geophys. Res.*, v. 64, n. 12, p. 2351-2355.
- Ludwig, W., Nafe, J. E., and Drake, C. L., 1970, Seismic refraction, *In: The Sea*, A. E. Maxwell (editor), vol. 4, Part I, New York, Wiley-Interscience, p. 53-84.
- Oliver, H. W., 1973, Principal facts, plots, and reduction for 1753 gravity stations in the Southern Sierra Nevada and Vicinity, California: NTIS pub #PB 231 185, U. S. Dept. of Commerce, Washington, D. C.
- Oliver, H. W., Griscom, A., Robbins, S. L., Hanna, W. F., 1969, U. S. Geological Survey Gravity data in California, part IV: U. S. Geol. Survey, Internal report, Menlo Park, California.
- Plouff, D., 1977a, Preliminary documentation for a FORTRAN program to compute gravity terrain corrections based on topography digitized on a geographic grid: U. S. Geol. Survey, Open-file report, no. 77-535, U. S. Govt. Printing Office, Washington, D. C.
- Plouff, D., 1977b, Gravity observations near McDermitt, Nevada during 1976: U. S. Geol. Survey, open-file report, no. 77-536, 13 p., U. S. Govt. Printing Office, Washington, D. C.
- Scheibe, D. M., and Howard, H. W., 1964, Classical methods for reduction of gravity observation: U. S. Air Force, Aeronautical Chart and Information Center Ref., Pub. 12, 65 p.
- Swick, C. H., 1942, Pendulum gravity measurements and isostatic reductions: U. S. Coast and Geod. Survey, Spec. Pub., no. 232, 82 p.
- Thiruvathukal, J. T., 1968, Regional Gravity of Oregon: unpub. Ph.D. Dissertation, Oregon State University, Corvallis, Oregon, 92 p.
- Wise, W. S., 1969, Geology and Petrology of the Mt. Hood Area: A study of High Cascade Volcanism, *Geo. Soc. of Am. Bull.*, v. 80, p. 969-1006.
- Woollard, G. P., Rose, J. C., 1963, International gravity measurements: Society of Exploration Geophysics, Tulsa, OK, 518 p.

APPENDIX

THEORETICAL GRAVITY, IUGG 1930 INTERNATIONAL GRAVITY FORMULA

EXPLANATION OF SYMBOLS: ID - STATION IDENTIFICATION, LAT - LATITUDE, LONG - LONGITUDE, ELEV - ELEVATION (FEET),
 OG - OBSERVED GRAVITY, THG - THEORETICAL GRAVITY, HTC - HAND TERRAIN CORRECTION, TTC - TOTAL TERRAIN CORRECTION,
 CC - CURVATURE CORRECTION, FAA - FREEAIR ANOMALY, CBA1, CBA2 - VARIABLE DENSITY COMPLETE BOUGUER ANOMALIES.
 GRAVITY DATA, ANOMALIES, AND CORRECTIONS IN MGALS. ESTIMATED UNCERTAINTIES, FAA +/- 1.0 MGL, CBA +/- 1.5 MGL.
 CBA1 REDUCTION DENSITY = 2.67 GM / CC CBA2 REDUCTION DENSITY = 2.27 GM / CC

ID	LAT	LONG	ELEV	OG	THG	HTC	TTC	CC	FAA	CBA1	CBA2	ID
MHL 3	45 20.61	-121 56.46	1425.0	980489.14	980660.39	0.00	4.85	0.57	-37.25	-81.57	-74.93	MHL 3
MHL 6	45 18.28	-121 45.27	3880.0	980328.18	980656.89	0.00	3.39	1.24	36.09	-94.89	-74.59	MHL 6
MHL 7	45 18.50	-121 42.29	4900.0	980260.54	980657.22	0.00	6.64	1.40	63.99	-97.99	-73.64	MHL 7
MHL 8	45 19.87	-121 42.16	5950.0	980190.14	980659.20	0.00	12.46	1.49	90.19	-101.77	-73.01	MHL 8
MHS01	45 17.04	-121 42.53	3652.0	980339.79	980655.03	0.00	3.11	1.19	28.13	-94.51	-76.14	MHS01
MHS02	45 25.46	-121 34.69	3060.0	980393.11	980667.69	0.08	5.51	1.06	13.14	-86.77	-71.81	MHS02
MHS03	45 30.39	-121 35.14	1831.0	980476.90	980675.10	0.02	2.77	0.71	-26.03	-86.41	-77.37	MHS03
MHS05	45 32.90	-121 42.03	1279.0	980513.34	980678.88	0.00	0.12	0.52	-45.27	-81.29	-75.89	MHS05
MHS06	45 13.07	-121 41.69	3874.0	980316.61	980649.06	0.00	3.47	1.24	31.79	-98.11	-78.65	MHS06
MH 01	45 19.96	-121 54.87	1577.0	980470.54	980659.42	0.00	6.71	0.62	-32.59	-80.28	-73.14	MH 01
MH 02	45 19.57	-121 54.42	1672.0	980472.62	980658.84	0.01	6.48	0.65	-28.99	-80.19	-72.52	MH 02
MH 03	45 19.01	-121 53.93	1804.0	980463.43	980657.99	0.00	6.49	0.70	-24.92	-80.66	-72.31	MH 03
MH 04	45 18.55	-121 52.88	1990.0	980451.92	980657.29	0.00	6.34	0.76	-18.24	-80.53	-71.20	MH 04
MH 05	45 18.43	-121 51.15	2294.0	980433.50	980657.12	0.00	5.41	0.85	-7.91	-81.59	-70.56	MH 05
MH 06	45 18.70	-121 50.04	2547.0	980416.69	980657.52	0.00	5.25	0.92	-1.34	-83.80	-71.52	MH 06
MH 07	45 18.85	-121 47.70	3120.0	980376.58	980657.75	2.38	9.06	1.07	12.19	-86.24	-71.49	MH 07
MH 08	45 18.80	-121 48.91	2806.0	980397.83	980657.67	0.01	4.05	0.99	4.00	-87.85	-74.09	MH 08
MH 09	45 18.46	-121 46.95	3501.0	980347.95	980657.15	0.00	3.30	1.18	27.49	-92.52	-74.54	MH 09
MH 10	45 15.55	-121 42.71	3420.0	980350.56	980652.78	0.00	3.60	1.14	19.34	-94.85	-77.74	MH 10
MH 11	45 14.48	-121 42.23	3550.0	980338.63	980651.16	0.20	3.21	1.17	21.25	-97.79	-79.96	MH 11
MH 12	45 13.55	-121 41.86	3952.0	980312.85	980649.77	0.02	2.82	1.25	34.65	-98.57	-78.62	MH 12
MH 13	45 11.65	-121 41.45	3826.0	980319.63	980646.91	0.01	1.64	1.23	32.44	-97.64	-78.15	MH 13
MH 14	45 17.33	-121 46.91	5027.0	980248.31	980655.46	7.77	14.33	1.41	65.45	-93.00	-69.33	MH 14
MH 15	45 17.63	-121 44.91	4656.0	980269.59	980655.91	10.32	14.23	1.37	51.41	-94.52	-72.66	MH 15
MH 16	45 18.04	-121 44.02	3925.0	980323.23	980656.53	0.00	4.09	1.25	35.73	-95.29	-75.66	MH 16
MH 17	45 17.24	-121 43.67	3030.0	980329.37	980655.32	0.00	2.94	1.23	34.15	-94.77	-75.45	MH 17
MH 18	45 16.13	-121 44.15	3608.0	980342.11	980653.65	0.00	2.69	1.18	27.69	-93.06	-75.65	MH 18
MH 19	45 15.19	-121 44.21	4145.0	980305.66	980652.24	0.04	4.27	1.29	43.13	-95.26	-74.53	MH 19
MH 20	45 14.34	-121 48.79	4705.0	980270.47	980650.96	1.80	6.94	1.37	61.85	-93.05	-69.85	MH 20
MH 21	45 15.87	-121 50.48	5041.0	980243.93	980653.26	14.02	22.61	1.42	64.58	-86.16	-63.57	MH 21
MH 22	45 16.02	-121 53.06	4770.0	980265.45	980653.49	11.64	19.78	1.38	68.40	-83.89	-62.27	MH 22
MH 23	45 16.45	-121 53.49	4226.0	980307.14	980654.13	5.83	11.44	1.30	50.33	-83.66	-63.59	MH 23
MH 24	45 17.04	-121 54.33	4110.0	980317.37	980655.03	9.35	14.61	1.20	48.76	-70.89	-59.89	MH 24
MH 25	45 14.66	-121 50.30	4689.0	980276.16	980651.43	0.29	10.46	1.37	63.56	-85.28	-62.68	MH 25
MH 26	45 17.87	-121 53.05	1846.0	980458.28	980656.27	0.00	8.62	0.71	-24.48	-79.46	-71.21	MH 26

ID	LAT	LONG	ELEV	OG	THG	HTC	TTC	CC	FNA	CBA1	CBA2	ID
MH 27	45 17.11	-121 51.25	2114.0	980436.04	980655.13	9.35	14.18	0.80	-20.30	-79.02	-70.23	MH 27
MH 28	45 16.41	-121 50.23	2308.0	980412.29	980654.00	10.31	14.42	0.80	-18.00	-85.63	-75.50	MH 28
MH 29	45 16.04	-121 48.40	2893.0	980381.40	980653.51	9.69	12.76	1.02	-0.09	-87.02	-74.00	MH 29
MH 30	45 16.38	-121 46.46	3188.0	980366.94	980654.03	0.02	6.00	1.09	12.66	-91.00	-75.54	MH 30
MH 31	45 16.96	-121 44.80	3531.0	980348.86	980654.98	0.03	4.70	1.17	25.95	-90.94	-73.43	MH 31
MH 32	45 14.80	-121 47.17	4457.0	980290.04	980651.78	0.05	4.60	1.34	58.09	-90.66	-68.38	MH 32
MH 33	45 13.64	-121 46.21	3467.0	980349.19	980649.90	0.03	1.84	1.15	25.26	-92.30	-74.69	MH 33
MH 34	45 12.43	-121 41.86	4024.0	980306.68	980648.09	0.18	2.39	1.26	36.92	-99.19	-78.80	MH 34
MH 35	45 11.56	-121 42.97	3573.0	980333.20	980646.77	0.04	2.87	1.18	22.37	-97.80	-79.79	MH 35
MH36A	45 19.16	-121 41.15	4799.0	980266.09	980658.22	0.02	7.08	1.39	59.84	-98.14	-74.47	MH36A
MH 37	45 17.53	-121 48.63	4414.0	980296.28	980653.76	0.10	7.64	1.33	55.51	-88.73	-67.12	MH 37
MH 38	45 12.02	-121 44.12	3879.0	980314.95	980647.47	0.02	1.98	1.24	32.19	-99.37	-79.66	MH 38
MH 39	45 12.66	-121 43.17	3931.0	980311.77	980648.44	0.03	4.24	1.25	32.93	-98.15	-78.52	MH 39
MH 40	45 11.99	-121 46.07	3844.0	980316.91	980647.42	0.00	1.79	1.23	30.91	-99.64	-80.00	MH 40
MH 41	45 11.22	-121 47.44	3969.0	980305.82	980646.27	0.01	1.82	1.25	32.72	-102.09	-81.89	MH 41
MH 42	45 12.13	-121 49.75	3588.0	980337.61	980647.63	0.04	3.79	1.18	27.33	-92.44	-74.49	MH 42
MH 43	45 11.92	-121 51.26	3223.0	980339.28	980647.31	0.49	3.42	1.10	15.01	-92.59	-76.47	MH 43
MH 44	45 11.81	-121 54.54	4088.0	980308.14	980647.15	0.01	3.66	1.28	45.34	-91.70	-71.17	MH 44
MH 45	45 13.69	-121 56.01	4877.0	980246.39	980649.99	19.49	27.61	1.40	54.91	-85.22	-64.22	MH 45
MH 46	45 12.58	-121 47.54	3586.0	980335.40	980648.31	0.42	3.05	1.18	24.25	-96.10	-78.14	MH 46
MH 47	45 13.06	-121 49.51	3236.0	980366.97	980649.04	0.11	2.22	1.10	22.19	-87.06	-70.69	MH 47
MH 48	45 13.00	-121 51.31	2867.0	980403.41	980648.95	0.19	3.22	1.01	24.04	-71.54	-57.22	MH 48
MH 49	45 13.80	-121 52.26	2710.0	980405.18	980650.15	0.46	4.50	0.97	9.84	-79.05	-65.74	MH 49
MH 50	45 14.48	-121 52.63	2655.0	980411.70	980651.05	0.03	4.69	0.95	10.38	-76.52	-63.51	MH 50
MH 51	45 15.01	-121 53.85	2492.0	980424.10	980651.97	0.62	5.23	0.91	6.46	-74.22	-62.13	MH 51
MH 52	45 15.65	-121 54.93	1773.0	980461.83	980652.93	0.00	9.54	0.69	-24.38	-76.00	-68.27	MH 52
MH 53	45 13.03	-121 39.95	5294.0	980219.99	980648.99	0.01	11.68	1.44	68.69	-101.64	-76.12	MH 53
MH 54	45 17.04	-121 35.57	5724.0	980196.95	980655.02	11.33	19.71	1.40	80.03	-96.96	-70.45	MH 54
MH 55	45 18.18	-121 33.47	4465.0	980294.61	980656.73	0.00	7.07	1.34	57.66	-88.89	-66.94	MH 55
MH 56	45 18.17	-121 31.74	5125.0	980259.31	980656.73	0.01	6.13	1.42	84.39	-85.70	-68.22	MH 56
MH 57	45 15.79	-121 35.52	5600.0	980202.62	980653.15	10.26	10.55	1.47	75.92	-98.00	-71.94	MH 57
MH 58	45 14.50	-121 34.50	4865.0	980256.01	980651.23	0.01	4.90	1.39	62.18	-100.24	-75.91	MH 58
MH 59	45 12.77	-121 35.02	4342.0	980286.34	980648.59	0.00	5.66	1.32	45.97	-97.78	-76.24	MH 59
MH 60	45 11.40	-121 34.43	3705.0	980327.53	980646.53	0.00	2.41	1.20	29.36	-95.79	-77.04	MH 60
MH 61	45 11.13	-121 32.51	3326.0	980350.38	980646.13	0.01	1.73	1.12	16.97	-95.86	-78.96	MH 61
MH 62	45 11.93	-121 38.04	3702.0	980325.37	980647.34	0.04	2.69	1.20	26.10	-98.68	-79.98	MH 62
MH 63	45 12.40	-121 32.76	3849.0	980319.26	980648.05	0.01	2.25	1.23	33.10	-97.16	-77.65	MH 63
MH 64	45 13.79	-121 31.91	4584.0	980274.10	980650.13	0.01	4.36	1.36	54.94	-98.40	-75.43	MH 64
MH 65	45 15.15	-121 32.88	5385.0	980222.00	980652.17	0.01	9.53	1.45	76.07	-99.51	-73.21	MH 65
MH 66	45 16.35	-121 32.35	5279.0	980237.08	980653.98	0.00	7.55	1.44	79.38	-94.56	-68.50	MH 66
MH 67	45 12.66	-121 28.29	3333.0	980348.95	980648.44	0.03	2.04	1.12	13.09	-98.07	-81.97	MH 67
MH 68	45 13.86	-121 29.49	3611.0	980337.17	980650.23	0.02	2.94	1.18	26.45	-94.95	-76.77	MH 68
MH 69	45 14.78	-121 29.34	4011.0	980316.10	980651.62	0.02	3.39	1.26	41.67	-93.00	-72.83	MH 69

ID	LAT	LONG	ELEV	OG	THG	HTC	TTC	CC	FAA	CBA1	CBA2	ID
MH 70	45 14.97	-121 26.52	3003.0	980375.78	980651.91	0.01	2.29	1.04	6.23	-94.94	-79.79	MH 70
MH 71	45 13.66	-121 26.51	2905.0	980376.97	980649.94	0.01	1.80	1.02	0.18	-98.12	-83.39	MH 71
MH 72	45 11.40	-121 27.01	2783.0	980382.91	980646.55	0.01	1.37	0.99	-1.96	-96.49	-82.33	MH 72
MH 73	45 16.68	-121 41.57	4067.0	980315.79	980654.47	0.10	2.90	1.27	43.69	-93.39	-72.06	MH 73
MH 74	45 18.17	-121 40.35	4250.0	980309.57	980656.72	0.01	4.07	1.30	52.43	-89.76	-68.46	MH 74
MH 75	45 18.63	-121 38.51	4674.0	980282.32	980657.41	0.03	4.55	1.37	64.34	-91.90	-68.49	MH 75
MH 76	45 19.80	-121 35.08	3793.0	980340.42	980659.10	0.00	5.22	1.22	37.06	-87.50	-68.72	MH 76
MH 78	45 17.47	-121 38.55	3856.0	980332.19	980655.67	0.28	4.15	1.23	39.06	-89.54	-78.27	MH 78
MH 79	45 17.03	-121 36.97	3565.0	980344.10	980655.01	0.16	6.58	1.18	26.16	-98.71	-73.20	MH 79
MH 80	45 14.30	-121 36.79	3449.0	980342.58	980650.90	0.01	3.15	1.15	15.96	-99.67	-82.35	MH 80
MH 81	45 12.81	-121 36.78	2970.0	980373.34	980648.66	0.00	6.36	1.04	3.94	-92.03	-77.65	MH 81
MH 82	45 11.32	-121 37.18	3452.0	980344.27	980646.42	0.03	2.01	1.15	22.42	-94.46	-76.95	MH 82
MH 83	45 14.02	-121 39.37	3283.0	980356.31	980651.68	0.01	5.62	1.11	13.31	-94.15	-78.06	MH 83
MH 84	45 15.98	-121 40.31	3639.0	980339.89	980653.43	0.00	4.68	1.19	28.68	-92.02	-73.95	MH 84
MH 85	45 20.13	-121 42.69	6277.0	980166.97	980659.68	0.01	13.85	1.51	97.36	-104.39	-74.17	MH 85
MH 86	45 20.48	-121 42.67	6635.0	980148.19	980660.19	0.09	17.93	1.52	103.78	-106.19	-74.74	MH 86
MH 87	45 20.71	-121 42.64	6980.0	980114.93	980660.55	0.05	19.83	1.52	110.49	-109.26	-76.34	MH 87
MH 88	45 20.91	-121 42.53	7282.0	980093.72	980660.85	0.13	23.46	1.51	117.35	-109.06	-75.14	MH 88
MH 90	45 21.32	-121 42.36	8068.0	980043.72	980661.46	7.55	33.61	1.46	140.58	-102.45	-66.04	MH 90
MH 91	45 21.51	-121 42.28	8484.0	980007.86	980661.76	0.19	39.68	1.42	143.51	-107.68	-70.05	MH 91
MH 92	45 22.70	-121 54.50	1947.0	980474.22	980663.54	0.01	4.48	0.74	-6.24	-68.91	-59.52	MH 92
MH 93	45 23.02	-121 52.79	2055.0	980453.72	980664.02	0.08	7.68	0.78	-17.06	-80.33	-70.85	MH 93
MH 94	45 23.61	-121 51.90	2389.0	980419.59	980664.90	0.22	6.73	0.80	-20.67	-96.30	-84.97	MH 94
MH 95	45 24.49	-121 50.78	2657.0	980416.55	980666.23	0.27	5.35	0.95	0.15	-86.00	-73.16	MH 95
MH 96	45 25.24	-121 49.32	3118.0	980387.61	980667.37	0.13	3.49	1.07	13.41	-90.51	-74.94	MH 96
MH 97	45 25.80	-121 47.73	3225.0	980367.07	980668.20	0.09	4.45	1.10	2.90	-103.75	-87.77	MH 97
MH 98	45 22.60	-121 49.75	2582.0	980421.09	980663.39	0.03	5.23	0.93	0.48	-83.29	-78.74	MH 98
MH 99	45 24.19	-121 48.04	3011.0	980340.60	980665.77	0.02	7.45	1.22	33.14	-90.62	-72.08	MH 99
MH100	45 26.47	-121 47.52	2909.0	980401.24	980669.21	2.77	6.57	1.02	5.55	-88.11	-74.00	MH100
MH101	45 27.01	-121 46.60	2399.0	980434.24	980671.22	0.08	4.66	0.88	-11.40	-89.45	-77.75	MH101
MH102	45 29.10	-121 45.72	2156.0	980449.83	980673.16	0.06	6.28	0.81	-20.60	-80.66	-78.47	MH102
MH103	45 29.91	-121 44.61	2323.0	980444.34	980674.39	0.13	4.83	0.86	-11.62	-86.00	-75.61	MH103
MH105	45 20.55	-121 53.03	4460.0	980285.53	980660.30	14.19	22.29	1.34	45.29	-86.15	-66.46	MH105
MH106	45 21.06	-121 53.53	4564.0	980274.74	980661.07	16.79	27.42	1.35	42.76	-86.04	-67.42	MH106
MH107	45 19.67	-121 51.93	4017.0	980324.07	980650.99	0.04	8.00	1.26	42.76	-86.71	-67.31	MH107
MH108	45 19.50	-121 51.36	3306.0	980374.48	980650.73	0.04	4.12	1.12	26.59	-83.16	-66.72	MH108
MH109	45 20.34	-121 50.82	3753.0	980346.88	980659.99	0.07	4.74	1.21	39.75	-84.72	-66.07	MH109
MH110	45 20.63	-121 49.47	3995.0	980333.41	980660.42	0.06	5.54	1.26	40.59	-83.30	-63.61	MH110
MH111	45 21.02	-121 50.98	4877.0	980265.86	980661.01	9.86	10.92	1.40	63.35	-85.46	-63.17	MH111
MH112	45 21.05	-121 48.86	4971.0	980260.32	980661.05	11.80	19.84	1.41	66.60	-84.51	-61.87	MH112
MH113	45 20.29	-121 43.00	5744.0	980206.00	980659.92	0.05	11.41	1.40	86.06	-99.92	-72.05	MH113
MH114	45 20.98	-121 44.70	5764.0	980200.90	980660.95	0.08	14.45	1.40	89.01	-93.02	-66.31	MH114
MH115	45 21.69	-121 44.85	5686.0	980211.57	980662.02	0.14	14.73	1.40	84.00	-96.59	-69.53	MH115

ID	LAT	LONG	ELEV	OG	THG	HTC	TTC	CC	FAA	CBA1	CBA2	ID
MH116	45 22.87	-121 45.78	4451.0	980297.07	980662.59	0.22	10.20	1.34	52.94	-90.00	-68.59	MH116
MH117	45 22.77	-121 47.81	3299.0	980373.28	980663.64	0.06	7.09	1.11	19.75	-86.00	-70.84	MH117
MH118	45 23.48	-121 48.63	2739.0	980412.88	980664.71	0.01	5.17	0.98	5.71	-83.51	-70.14	MH118
MH119	45 19.20	-121 46.86	3866.0	980329.67	980658.27	0.02	4.48	1.22	29.24	-97.31	-78.35	MH119
MH120	45 19.30	-121 43.89	4997.0	980252.68	980658.43	0.09	7.26	1.41	64.03	-100.55	-75.98	MH120
MH121	45 26.47	-121 35.66	3169.0	980386.08	980669.22	0.02	4.13	1.08	14.75	-90.29	-74.56	MH121
MH122	45 27.57	-121 35.83	2787.0	980411.89	980670.87	0.01	3.88	0.99	3.07	-89.89	-75.96	MH122
MH123	45 28.16	-121 35.13	2510.0	980430.47	980671.76	0.01	2.79	0.91	-5.28	-89.01	-76.46	MH123
MH124	45 29.63	-121 35.12	2026.0	980464.33	980573.97	0.01	2.74	0.77	-19.13	-86.26	-76.20	MH124
MH125	45 32.18	-121 31.87	3779.0	980358.57	980677.79	4.75	10.66	1.22	36.08	-83.37	-65.47	MH125
MH126	45 30.32	-121 29.34	3954.0	980350.01	980675.00	0.00	3.96	1.25	46.76	-85.39	-65.60	MH126
MH127	45 29.80	-121 26.90	3370.0	980390.35	980674.34	0.04	3.68	1.13	32.86	-79.53	-62.69	MH127
MH128	45 29.66	-121 30.65	3986.0	980344.91	980674.01	0.00	4.34	1.26	45.66	-87.20	-67.30	MH128
MH129	45 27.87	-121 31.60	4444.0	980383.51	980671.31	0.53	11.07	1.33	50.01	-91.83	-70.50	MH129
MH130	45 25.24	-121 31.22	4316.0	980316.84	980667.35	0.00	3.74	1.31	55.26	-89.52	-67.83	MH130
MH131	45 24.55	-121 32.91	4230.0	980321.00	980666.32	0.02	4.07	1.30	53.18	-88.32	-67.12	MH131
MH132	45 27.77	-121 37.52	2845.0	980409.29	980671.17	0.00	3.43	1.00	5.63	-88.98	-74.80	MH132
MH133	45 26.05	-121 40.07	3589.0	980356.46	980668.58	0.26	8.04	1.18	25.33	-90.22	-72.91	MH133
MH134	45 27.01	-121 39.64	3590.0	980357.46	980678.02	0.22	5.18	1.18	24.97	-93.47	-75.72	MH134
MH135	45 26.85	-121 41.81	3670.0	980352.84	980669.78	0.01	4.46	1.20	28.11	-93.79	-75.53	MH135
MH136	45 26.56	-121 43.25	4747.0	980279.89	980669.35	0.30	8.47	1.38	56.82	-97.99	-74.80	MH136
MH137	45 26.79	-121 31.36	4912.0	980274.62	980669.69	9.21	16.50	1.40	66.72	-85.71	-62.87	MH137
MH138	45 26.65	-121 27.81	3632.0	980364.48	980669.47	0.01	2.75	1.19	36.49	-85.82	-67.50	MH138
MH139	45 26.34	-121 29.37	3449.0	980376.63	980669.01	0.08	4.79	1.15	31.90	-82.89	-65.82	MH139
MH140	45 27.77	-121 29.21	3448.0	980376.33	980671.16	0.03	2.81	1.15	29.36	-86.58	-69.21	MH140
MH141	45 28.83	-121 27.57	3030.0	980487.71	980672.77	0.07	2.95	1.05	19.84	-81.69	-66.41	MH141
MH142	45 27.20	-121 26.34	3258.0	980389.53	980670.31	0.02	2.03	1.11	25.55	-84.64	-68.13	MH142
MH143	45 24.63	-121 28.85	4627.0	980295.56	980666.44	0.02	6.37	1.36	64.12	-88.68	-65.79	MH143
MH144	45 23.81	-121 24.60	3475.0	980377.45	980665.21	0.01	2.10	1.15	38.97	-78.61	-68.99	MH144
MH145	45 22.79	-121 26.78	3683.0	980358.92	980663.67	0.03	3.84	1.20	41.53	-81.44	-63.82	MH145
MH146	45 23.15	-121 28.66	4561.0	980382.79	980664.22	0.04	4.51	1.35	67.38	-85.83	-62.19	MH146
MH147	45 21.84	-121 26.41	4309.0	980319.89	980661.03	0.01	4.02	1.31	63.17	-81.00	-59.47	MH147
MH148	45 19.08	-121 27.92	5651.0	980218.77	980658.89	6.85	16.73	1.47	91.91	-85.57	-58.98	MH148
MH149	45 20.31	-121 27.52	4753.0	980287.60	980659.94	0.28	5.92	1.38	74.51	-83.86	-59.45	MH149
MH150	45 21.54	-121 29.07	5217.0	980258.67	980661.80	0.02	6.22	1.43	87.33	-85.82	-59.88	MH150
MH151	45 20.56	-121 31.38	6525.0	980157.61	980660.31	9.41	23.33	1.51	110.66	-90.87	-60.00	MH151
MH152	45 22.92	-121 32.11	5143.0	980257.45	980663.87	0.01	6.98	1.43	77.88	-92.77	-67.33	MH152
MH153	45 25.43	-121 36.73	3982.0	980334.81	980667.64	0.10	4.88	1.26	41.56	-98.63	-78.83	MH153
MH154	45 25.47	-121 38.83	4588.0	980291.86	980667.70	0.05	7.40	1.36	54.70	-95.74	-73.20	MH154
MH155	45 24.93	-121 38.19	4811.0	980278.80	980666.89	0.02	7.31	1.39	63.41	-94.76	-71.86	MH155
MH156	45 24.80	-121 38.80	5718.0	980213.74	980665.49	0.01	10.92	1.48	85.78	-99.80	-72.80	MH156
MH157	45 31.66	-121 37.80	1660.0	980488.61	980677.03	0.09	2.98	0.65	-32.32	-86.69	-78.54	MH157
MH158	45 27.98	-121 39.77	3837.0	980341.12	980671.48	0.02	8.18	1.23	30.39	-93.52	-74.96	MH158

ID	LAT	LONG	ELEV	OG	THG	HTC	TTC	CC	FAA	CBA1	CBA2	ID
MH159	45 28.93	-121 39.39	3204.0	980385.83	980672.92	0.04	3.35	1.09	14.17	-92.85	-76.82	MH159
MH160	45 29.43	-121 38.18	2678.0	980420.87	980673.66	0.00	2.96	0.96	-1.74	-90.88	-77.46	MH160
MH161	45 30.09	-121 39.98	3212.0	980389.21	980674.65	0.00	3.19	1.09	16.57	-90.89	-74.79	MH161
MH162	45 29.56	-121 40.72	3726.0	980354.94	980673.86	0.00	4.88	1.21	31.40	-92.89	-73.59	MH162
MH163	45 27.93	-121 42.80	4450.0	980383.22	980671.40	0.01	6.61	1.34	50.19	-96.31	-74.36	MH163
MH164	45 29.51	-121 42.25	3636.0	980362.44	980673.79	0.05	3.64	1.19	30.51	-91.85	-72.84	MH164
MH165	45 28.52	-121 43.74	4378.0	980386.85	980672.38	0.03	9.14	1.32	46.15	-95.33	-74.15	MH165
MH166	45 30.87	-121 42.77	3778.0	980358.76	980675.83	0.26	9.96	1.22	30.14	-89.97	-71.98	MH166
MH167	45 27.66	-121 44.37	3975.0	980331.21	980671.00	0.21	6.05	1.26	33.94	-96.84	-77.25	MH167
MH168	45 26.44	-121 46.24	2615.0	980417.68	980669.16	0.01	6.68	0.94	-5.68	-89.21	-76.78	MH168
MH169	45 29.39	-121 36.31	2234.0	980449.84	980673.61	0.02	2.86	0.83	-14.58	-88.67	-77.56	MH169
MH170	45 24.15	-121 46.49	4591.0	980283.13	980665.73	11.38	17.14	1.36	49.83	-91.77	-78.68	MH170
MH171	45 24.91	-121 47.58	4534.0	980288.49	980666.87	10.78	16.48	1.35	47.89	-91.62	-78.72	MH171
MH172	45 28.91	-121 48.81	3148.0	980395.81	980672.89	0.01	3.03	1.08	18.91	-86.51	-78.71	MH172
MH173	45 28.17	-121 47.56	3818.0	980338.67	980671.77	14.18	17.81	1.22	25.11	-89.85	-71.94	MH173
MH174	45 30.85	-121 46.67	2651.0	980425.62	980675.79	0.01	3.91	0.95	-8.91	-88.37	-75.26	MH174
MH175	45 29.76	-121 47.68	4468.0	980296.43	980674.15	12.16	19.57	1.34	42.34	-91.82	-71.72	MH175
MH176	45 28.68	-121 36.89	5868.0	980256.98	980668.58	0.02	6.88	1.42	72.18	-95.73	-78.58	MH176
MH177	45 21.51	-121 36.21	4881.0	980276.48	980661.76	0.17	6.56	1.39	66.88	-92.57	-68.81	MH177
MH178	45 22.86	-121 35.67	4169.0	980328.62	980663.79	0.89	6.66	1.29	48.79	-88.83	-67.53	MH178
MH179	45 23.96	-121 35.49	3744.0	980354.68	980665.43	0.48	5.98	1.21	41.26	-81.66	-63.25	MH179
MH180	45 19.38	-121 38.80	4472.0	980292.79	980658.54	0.88	4.56	1.34	54.68	-94.62	-72.25	MH180
MH181	45 19.18	-121 33.59	5916.0	980195.45	980658.12	10.28	19.68	1.49	93.47	-90.19	-62.68	MH181
MH182	45 19.87	-121 31.47	3899.0	980341.48	980658.87	0.03	7.27	1.24	49.91	-77.84	-58.82	MH182
MH183	45 19.88	-121 38.30	3586.0	980358.75	980658.89	3.52	7.91	1.18	37.83	-77.75	-68.43	MH183
MH184	45 18.88	-121 29.96	3424.0	980368.88	980657.67	3.56	8.19	1.14	32.27	-77.47	-61.83	MH184
MH185	45 17.49	-121 28.88	3849.0	980386.84	980655.71	0.87	8.55	1.86	17.82	-78.68	-64.22	MH185
MH186	45 17.88	-121 27.95	2848.0	980397.48	980655.88	0.18	8.57	1.88	18.11	-79.46	-66.84	MH186
MH187	45 16.12	-121 26.36	2549.0	980489.29	980653.64	0.28	7.68	0.92	-4.67	-84.93	-72.91	MH187
MH188	45 16.37	-121 29.87	4378.0	980299.25	980654.82	8.37	4.24	1.32	56.88	-98.85	-68.16	MH188
MH189	45 15.44	-121 29.34	4261.0	980299.97	980652.62	0.82	3.93	1.31	47.96	-94.75	-73.37	MH189
MH190	45 19.97	-121 39.86	5358.0	980229.32	980659.44	0.01	8.81	1.45	73.59	-181.79	-73.52	MH190
MH191	45 21.83	-121 39.44	5558.0	980215.57	980661.83	0.28	12.91	1.47	76.29	-181.56	-74.91	MH191
MH192	45 21.14	-121 37.99	5656.0	980213.87	980661.19	0.05	8.57	1.47	83.59	-182.22	-74.39	MH192
MH193	45 21.56	-121 38.74	6633.0	980148.46	980661.82	9.97	22.82	1.52	182.15	-182.78	-72.88	MH193
MH194	45 22.43	-121 39.58	7368.0	980896.09	980663.13	8.39	22.73	1.51	124.78	-185.82	-78.68	MH194
MH195	45 23.41	-121 39.48	6658.0	980146.84	980664.68	0.12	16.72	1.52	187.34	-184.26	-72.56	MH195
MH196	45 31.43	-121 34.88	1649.0	980493.41	980676.68	0.88	3.41	0.65	-28.21	-81.68	-73.67	MH196
MH197	45 29.86	-121 33.68	1831.0	980478.63	980674.31	0.82	5.71	0.71	-23.51	-88.96	-72.35	MH197
MH198	45 27.89	-121 34.12	2157.0	980452.56	980671.34	0.83	6.23	0.81	-15.95	-84.18	-73.89	MH198
MH199	45 26.77	-121 34.67	2481.0	980434.28	980669.66	0.83	8.16	0.88	-9.61	-84.23	-73.85	MH199
MH200	45 23.78	-121 34.14	3875.0	980391.24	980665.84	0.86	9.83	1.86	15.33	-81.58	-67.86	MH200
MH201	45 22.45	-121 33.96	3385.0	980364.42	980663.16	0.82	7.46	1.12	12.81	-94.37	-78.44	MH201

ID	LAT	LONG	ELEV	OG	THG	HTC	TTC	CC	FAA	CBA1	CBA2	ID
MH202	45 20.37	-121 34.19	3558.0	980357.88	980660.04	0.01	7.85	1.17	32.37	-82.30	-65.12	MH202
MH203	45 31.19	-121 36.52	1704.0	980485.98	980676.32	0.01	2.43	0.67	-30.10	-86.46	-78.01	MH203
MH204	45 30.70	-121 40.99	2803.0	980416.45	980675.69	0.28	5.24	0.99	4.32	-87.84	-73.35	MH204
MH205	45 30.52	-121 50.08	4057.0	980334.62	980675.30	16.04	20.01	1.27	40.75	-78.08	-68.96	MH205
MH206	45 24.20	-121 39.90	5994.0	980192.55	980665.80	0.31	15.28	1.58	90.22	-100.43	-71.87	MH206
MH207	45 24.34	-121 41.45	5915.0	980198.93	980666.00	0.00	13.85	1.49	88.98	-100.40	-72.03	MH207
MH208	45 24.84	-121 41.87	5828.0	980203.62	980666.76	0.00	15.23	1.49	84.73	-100.38	-72.58	MH208
MH209	45 24.76	-121 43.01	5653.0	980217.43	980666.64	0.13	12.82	1.47	82.21	-99.25	-72.06	MH209
MH210	45 24.16	-121 43.89	5579.0	980221.75	980665.73	0.10	14.12	1.47	80.49	-97.14	-70.53	MH210
MH211	45 21.37	-121 51.86	3066.0	980389.96	980661.53	0.12	6.40	1.06	16.71	-92.52	-67.65	MH211
MH212	45 22.49	-121 51.49	2450.0	980427.46	980663.23	0.58	6.61	0.90	-5.48	-83.24	-71.58	MH212
MH213	45 23.53	-121 49.91	2895.0	980401.58	980664.79	0.05	4.85	1.02	9.00	-85.91	-71.69	MH213
MH214	45 24.01	-121 53.99	2571.0	980421.18	980665.51	0.20	4.01	0.93	-2.58	-87.19	-74.51	MH214
MH215	45 24.80	-121 52.53	2943.0	980399.69	980666.70	0.08	3.80	1.03	9.71	-87.90	-73.27	MH215
MH216	45 25.75	-121 51.35	3633.0	980357.57	980660.12	0.01	2.73	1.19	31.03	-91.34	-73.01	MH216
MH217	45 26.99	-121 53.86	2791.0	980414.86	980669.99	0.06	2.38	0.99	7.30	-86.50	-72.45	MH217
MH218	45 26.03	-121 52.00	3043.0	980396.06	980660.54	0.03	4.32	1.05	13.64	-86.88	-71.83	MH218
MH219	45 27.04	-121 52.38	2938.0	980404.65	980670.06	0.19	3.42	1.03	10.84	-86.98	-72.32	MH219
MH220	45 28.43	-121 54.16	2739.0	980421.70	980672.15	0.01	2.58	0.98	7.09	-84.72	-70.97	MH220
MH221	45 28.71	-121 52.73	2622.0	980427.01	980672.58	0.09	4.78	0.94	0.97	-84.62	-71.80	MH221
MH222	45 29.52	-121 54.06	2409.0	980437.07	980673.00	0.01	3.39	0.91	-2.70	-85.10	-72.76	MH222
MH223	45 27.65	-121 50.64	3166.0	980392.23	980670.98	0.09	2.94	1.08	18.93	-87.19	-71.30	MH223
MH224	45 26.17	-121 49.87	4112.0	980324.46	980668.76	0.09	5.40	1.28	42.30	-93.02	-73.43	MH224
MH225	45 27.23	-121 48.32	4565.0	980204.17	980670.35	15.60	22.36	1.35	43.00	-91.69	-71.51	MH225
MH226	45 27.94	-121 49.43	4338.0	980308.38	980671.43	9.66	14.79	1.32	44.80	-89.68	-69.54	MH226
MH227	45 28.38	-121 50.06	4566.0	980291.15	980672.08	10.74	16.84	1.35	48.34	-91.98	-70.09	MH227
MH228	45 25.12	-121 46.11	2999.0	980388.93	980667.18	0.00	8.79	1.04	3.74	-90.00	-76.64	MH228
MH230	45 29.91	-121 50.65	2935.0	980405.07	980674.38	0.00	5.88	1.03	6.65	-88.60	-74.33	MH230
MH231	45 20.02	-121 46.70	4105.0	980311.17	980659.50	0.00	5.14	1.29	45.13	-93.76	-72.95	MH231
MH232	45 22.40	-121 41.69	11235.0	979763.58	980663.09	42.52	125.87	0.87	156.25	-101.94	-63.26	MH232
GS 1	45 18.10	-121 49.23	2790.0	980394.20	980656.74	0.89	7.37	0.99	-0.20	-88.98	-75.68	GS 1
GS 2	45 18.20	-121 43.16	4380.0	980292.94	980656.89	0.03	4.57	1.32	47.85	-98.30	-76.40	GS 2
GS 3	45 15.73	-121 38.39	4515.0	980203.25	980653.05	0.10	5.69	1.35	54.68	-94.97	-72.55	GS 3
GS 4	45 17.15	-121 40.26	4001.0	980320.43	980655.19	0.01	3.03	1.27	40.93	-88.50	-67.91	GS 4
GS 5	45 18.14	-121 36.13	4195.0	980306.98	980656.68	0.19	4.45	1.29	44.71	-95.21	-74.25	GS 5
GS 6	45 26.38	-121 37.40	3685.0	980357.47	980669.07	0.01	4.57	1.20	34.06	-87.45	-69.12	GS 6
GS 7	45 24.75	-121 36.23	3920.0	980339.03	980666.62	0.05	5.08	1.24	40.96	-88.98	-69.44	GS 7
GS 8	45 23.70	-121 29.90	4577.0	980301.26	980665.04	0.00	3.98	1.35	66.53	-86.95	-63.96	GS 8
GS 9	45 25.66	-121 32.86	3923.0	980339.45	980667.99	0.03	3.83	1.25	40.29	-90.92	-71.26	GS 9
GS10	45 26.46	-121 32.51	3730.0	980357.77	980669.19	0.01	4.07	1.21	39.27	-85.00	-66.45	GS10
GS11	45 21.38	-121 33.99	3445.0	980366.99	980661.55	0.00	6.93	1.15	29.35	-82.37	-65.63	GS11
GS12	45 17.50	-121 34.03	5220.0	980242.74	980655.71	0.39	6.52	1.44	77.76	-95.19	-69.28	GS12
GS13	45 18.41	-121 34.28	5585.0	980219.18	980657.00	0.38	10.61	1.47	87.13	-94.21	-67.04	GS13

MT HOOD GRAVITY DATA, 1977/1978 PAGE 7

ID	LAT	LONG	ELEV	OG	THG	HTC	TTC	CC	FAA	CBA1	CBA2	ID
GS14	45 20.00	-121 32.06	5220.0	980256.40	980659.48	0.01	7.07	1.44	07.66	-84.74	-58.91	GS14
GS15	45 22.05	-121 31.75	5495.0	980238.42	980662.56	0.01	8.40	1.46	92.44	-88.04	-61.00	GS15
GS16	45 21.40	-121 30.45	5685.0	980225.79	980661.70	0.00	8.37	1.48	98.52	-89.48	-60.47	GS16
GS17	45 23.82	-121 51.76	2870.0	980453.61	980664.02	0.00	5.15	0.78	-15.76	-82.00	-72.07	GS17
GS18	45 23.13	-121 50.33	2330.0	980437.13	980664.18	0.00	5.09	0.86	-7.96	-83.20	-71.93	GS18
GS19	45 23.03	-121 49.20	2940.0	980397.01	980664.03	0.25	4.69	1.03	10.21	-86.40	-71.93	GS19
GS20	45 21.43	-121 47.63	3230.0	980374.11	980661.63	4.76	8.86	1.10	16.18	-86.22	-70.88	GS20
GS21	45 23.79	-121 50.91	2540.0	980427.30	980665.18	0.02	3.92	0.92	0.95	-82.68	-70.15	GS21
GS22	45 24.44	-121 49.45	2900.0	980400.79	980666.16	0.12	4.69	1.02	7.31	-87.93	-73.66	GS22
GS23	45 24.06	-121 49.85	3410.0	980372.07	980665.58	0.57	5.33	1.14	27.98	-84.21	-67.41	GS23
GS24	45 24.19	-121 47.57	3865.0	980334.34	980665.78	0.33	6.54	1.23	31.95	-94.57	-75.62	GS24
GS25	45 23.28	-121 47.55	3015.0	980388.62	980664.41	0.39	6.34	1.05	7.78	-89.84	-75.23	GS25
GS26	45 23.75	-121 47.91	2020.0	980403.54	980665.12	0.00	5.00	1.00	3.58	-87.80	-74.11	GS26
GS27	45 23.43	-121 48.46	2750.0	980410.61	980664.63	0.00	5.31	0.98	4.55	-84.91	-71.51	GS27
GS28	45 19.11	-121 42.03	5220.0	980238.10	980658.14	0.38	7.94	1.44	70.78	-100.75	-75.05	GS28
GS29	45 18.79	-121 43.17	4920.0	980258.02	980657.65	0.01	6.59	1.40	62.91	-99.70	-75.34	GS29
GS30	45 16.02	-121 43.94	3620.0	980342.43	980654.69	0.00	2.54	1.19	20.10	-94.01	-75.72	GS30
GS31	45 17.91	-121 42.97	4192.0	980306.08	980656.33	0.03	3.94	1.29	43.07	-96.46	-75.43	GS31
GS32	45 17.63	-121 43.21	4040.0	980315.20	980655.91	0.05	3.56	1.27	39.13	-96.37	-76.07	GS32
N 1	45 19.85	-121 42.54	5910.0	980192.75	980659.25	0.01	11.35	1.49	89.08	-102.63	-73.91	N 1
N 2	45 19.90	-121 42.56	5949.0	980190.03	980659.32	0.04	11.66	1.49	89.95	-102.79	-73.91	N 2
N 3	45 19.94	-121 42.59	6004.0	980186.02	980659.38	0.04	12.17	1.50	91.04	-103.06	-73.90	N 3
N 4	45 19.99	-121 42.62	6041.0	980183.54	980659.46	0.05	12.50	1.50	91.97	-103.07	-73.85	N 4
N 5	45 20.03	-121 42.62	6101.0	980179.21	980659.52	0.16	12.89	1.50	93.22	-103.40	-74.01	N 5
N 6	45 20.07	-121 42.66	6148.0	980175.00	980659.58	0.08	13.07	1.50	94.24	-103.80	-74.20	N 6
N 7	45 20.11	-121 42.67	6190.0	980173.00	980659.65	0.11	13.24	1.50	95.24	-104.15	-74.28	N 7
N 8	45 20.15	-121 42.67	6229.0	980170.41	980659.71	0.07	13.38	1.51	96.25	-104.33	-74.28	N 8
N 9	45 20.20	-121 42.68	6274.0	980167.30	980659.78	0.11	13.72	1.51	97.30	-104.47	-74.24	N 9
N10	45 20.24	-121 42.68	6315.0	980164.54	980659.84	0.04	13.99	1.51	98.33	-104.57	-74.17	N10
N11	45 20.29	-121 42.70	6357.0	980161.59	980659.90	0.07	14.48	1.51	99.26	-104.58	-74.04	N11
N12	45 20.32	-121 42.70	6412.0	980157.52	980659.95	0.10	15.21	1.51	100.31	-104.68	-73.97	N12
N13	45 20.35	-121 42.71	6460.0	980153.95	980660.01	0.10	15.89	1.51	101.20	-104.75	-73.90	N13
N14	45 20.30	-121 42.72	6504.0	980150.69	980660.05	0.07	16.54	1.51	102.03	-104.77	-73.79	N14
N15	45 20.42	-121 42.74	6553.0	980147.00	980660.11	0.07	17.28	1.51	102.89	-104.85	-73.73	N15
N16	45 20.45	-121 42.77	6605.0	980142.95	980660.15	0.12	18.09	1.52	103.68	-105.02	-73.76	N16
N17	45 20.48	-121 42.78	6646.0	980139.00	980660.19	0.06	18.42	1.52	104.34	-105.43	-74.00	N17
N18	45 20.52	-121 42.76	6691.0	980136.50	980660.26	0.06	18.17	1.52	105.28	-106.28	-74.50	N18
N19	45 20.56	-121 42.76	6741.0	980132.90	980660.31	0.10	18.38	1.52	106.24	-106.81	-74.89	N19
N20	45 20.58	-121 42.76	6784.0	980129.68	980660.35	0.10	18.59	1.52	107.03	-107.20	-75.18	N20
N21	45 20.63	-121 42.75	6858.0	980124.62	980660.43	0.10	18.98	1.52	108.84	-107.60	-75.17	N21
S 1	45 19.86	-121 42.67	5932.0	980190.92	980659.27	0.04	11.65	1.49	89.30	-102.87	-74.00	S 1
S 2	45 19.82	-121 42.68	5886.0	980194.21	980659.21	0.04	11.19	1.49	88.32	-102.73	-74.10	S 2
S 3	45 19.79	-121 42.68	5854.0	980196.40	980659.16	0.05	10.90	1.49	87.56	-102.69	-74.19	S 3

MT HOOD GRAVITY DATA, 1977/1978 PAGE 8

ID	LAT	LONG	ELEV	OG	THG	HTC	TTC	CC	FRA	CBA1	CBA2	ID
S 4	45 19.75	-121 42.69	5804.0	980199.95	980659.89	0.06	10.51	1.48	86.47	-102.46	-74.15	S 4
S 5	45 19.70	-121 42.70	5759.0	980202.99	980659.03	0.06	10.26	1.48	85.35	-102.30	-74.18	S 5
S 6	45 19.66	-121 42.71	5696.0	980207.48	980658.96	0.07	10.04	1.48	83.99	-101.72	-73.90	S 6
S 7	45 19.62	-121 42.71	5648.0	980211.36	980658.90	0.07	9.95	1.47	82.67	-101.22	-73.67	S 7
S 8	45 19.57	-121 42.71	5582.0	980215.50	980658.83	0.05	9.93	1.47	81.43	-100.49	-73.24	S 8
S 9	45 19.52	-121 42.72	5541.0	980218.19	980658.75	0.07	9.86	1.46	80.34	-100.25	-73.19	S 9
S10	45 19.47	-121 42.73	5452.0	980223.92	980658.68	0.17	9.39	1.46	77.78	-100.24	-73.57	S10
S11	45 19.42	-121 42.73	5411.0	980226.70	980658.61	0.23	9.02	1.45	76.78	-100.20	-73.69	S11
S12	45 19.38	-121 42.74	5387.0	980228.33	980658.54	0.19	8.72	1.45	76.22	-100.24	-73.80	S12
S13	45 19.33	-121 42.76	5346.0	980231.06	980658.46	0.21	8.37	1.45	75.18	-100.24	-73.96	S13
S14	45 19.27	-121 42.76	5349.0	980230.50	980658.37	0.01	8.16	1.45	74.99	-100.74	-74.41	S14
E 1	45 19.99	-121 42.57	6022.0	980185.01	980659.47	0.05	12.19	1.50	91.64	-103.05	-73.88	E 1
E 2	45 19.98	-121 42.51	6019.0	980185.07	980659.45	0.05	12.12	1.50	91.44	-103.22	-74.06	E 2
E 3	45 20.01	-121 42.42	5990.0	980187.31	980659.49	0.15	12.15	1.50	90.91	-102.73	-73.72	E 3
E 4	45 20.03	-121 42.33	5977.0	980180.06	980659.52	0.50	12.76	1.49	90.41	-102.18	-73.33	E 4
E 5	45 20.01	-121 42.26	5951.0	980189.68	980659.50	0.01	12.30	1.49	89.61	-102.55	-73.76	E 5
E 6	45 20.02	-121 42.18	5939.0	980190.38	980659.50	0.03	12.23	1.49	89.18	-102.64	-73.91	E 6
W 1	45 19.98	-121 42.65	6050.0	980182.17	980659.44	0.05	12.86	1.50	92.21	-103.04	-73.79	W 1
W 2	45 19.99	-121 42.70	6071.0	980181.14	980659.46	0.05	13.04	1.50	92.38	-103.14	-73.85	W 2
W 3	45 20.00	-121 42.76	6003.0	980180.15	980659.47	0.05	13.21	1.50	92.51	-103.25	-73.92	W 3
W 4	45 20.01	-121 42.80	6072.0	980181.05	980659.50	0.05	12.87	1.50	92.35	-103.37	-74.05	W 4
W 5	45 20.03	-121 42.84	6067.0	980181.43	980659.52	0.11	12.83	1.50	92.23	-103.36	-74.06	W 5
W 6	45 20.04	-121 42.89	6044.0	980182.01	980659.53	0.12	12.62	1.50	90.65	-104.37	-75.15	W 6
W 7	45 20.04	-121 42.89	6045.0	980182.73	980659.54	0.05	12.56	1.50	91.45	-103.66	-74.43	W 7
W 8	45 20.05	-121 43.02	6057.0	980181.17	980659.55	0.05	12.55	1.50	91.01	-104.52	-75.23	W 8
W 9	45 20.06	-121 43.10	6033.0	980182.41	980659.57	0.22	12.61	1.50	89.98	-104.68	-75.51	W 9
W10	45 20.06	-121 43.16	6032.0	980182.13	980659.57	0.05	12.52	1.50	89.60	-105.11	-75.94	W10
GS33	45 19.71	-121 42.60	5776.0	980202.29	980659.04	0.12	10.37	1.48	86.23	-101.80	-73.70	GS33